OXFORD GENETICS

GENETICS, 2023, iyad056
https://doi.org/10.1093/genetics/iyad056
Advance Access Publication Date: 31 March 2023
Investigation

The frequency and differential pleiotropy of phenotypic nonspecificity in *Drosophila melanogaster*

Anthony Percival-Smith,* Sheng Cheng, Kassie Ouellette

Department of Biology, The University of Western Ontario, London, Ontario, Canada N6A 5B7

*Corresponding author: Department of Biology, The University of Western Ontario, London, Ontario, Canada N6A 5B7. Email: aperciva@uwo.ca

Abstract

The regulation of the initiation of transcription by transcription factors is often assumed to be dependent on specific recognition of DNA-binding sites and nonredundant. However, the redundant induction or rescue of a phenotype by transcription factors, phenotypic nonspecificity, challenges these assumptions. To assess the frequency of phenotypic nonspecificity in the rescue of transcription factor phenotypes, seven transcription factor phenotypes (labial, Deformed, Sex combs reduced, Ultrabithorax, fruitless, doublesex, and apterous) were screened for rescue by the expression of 12, or more, nonresident transcription factors. From 308 assessments of rescue by nonresident transcription factors, 18 rescues were identified across 6 of the 7 transcription factor phenotypes. Seventeen of the 18 rescues were with transcription factors that recognize distinct DNA-binding sites relative to the resident transcription factors. All rescues were nonuniform across pleiotropic transcription factor phenotypes suggesting extensive differential pleiotropy of the rescue. Primarily using RNAi to knockdown expression, and with the exceptions of the requirement of Bric a Brac 1 for female abdominal pigmentation and Myb oncogene-like for wing development, no evidence was found for a role of the other 16 nonresident transcription factor in the transcription factor phenotypes assessed. Therefore, these 16 rescues are likely due to functional complementation and not due to the expression of an epistatic function in the developmental/behavioral pathway. Phenotypic nonspecificity is both differentially pleiotropic and frequent, as on average 1 in 10–20 nonresident transcription factors rescue a phenotype. These observations will be important in future considerations of transcription factors function.

Keywords: transcription factors, gene expression, two step nuclear search, labial, Deformed, Sex combs reduced, Ultrabithorax, fruitless, doublesex, apterous

Introduction

A major mechanism controlling gene expression is the regulation of the rate of transcription initiation. The initiation rate is mediated by transcription factors (TFs) that bind to specific DNA-binding sites in gene regulatory sequences. The set of TFs expressed in a cell are responsible for the transcription of a unique set of genes that dictate the phenotype of a cell or group of cells. A common view of TF function is that the unique gene expression pattern of a cell is dependent on TFs binding specific *cis*-acting elements in the regulatory sequences of the expressed genes. Specific recruitment of TFs to the regulatory sequences of expressed genes is achieved through DNA-binding domains that recognize a specific DNA sequence together with specific cooperative protein–protein interactions such that a restricted set of genes are regulated to bring about a phenotype. For example, the yeast mating type TF α1 (MAT α1) in a cooperative interaction with MCM1 activates the expression of both the α pheromone and **a** pheromone receptor required for the α mating type phenotype (Bender and Sprague 1987). Based on a common assumption of phenotypic specificity of TF function, there is little expectation that the function of MAT α1 can be substituted by another *Saccharomyces cerevisiae*, nonresident TF (i.e. not MAT α1) that recognizes a distinct DNA-binding sequence and was not tested. This lack of experimental inquiry highlights the assumption made at the outset of analyses of TF function that TFs are unique, and self-contained, in terms of mechanisms employed to specifically bring about a phenotype.

Phenotypic specificity of TF function predicts limited redundancy of TF function, and testing this expectation uncovered extensive phenotypic nonspecificity (redundancy) of TF function (Percival-Smith 2017, 2018). Phenotypic nonspecificity of TF function is multiple TFs inducing or rescuing a phenotype. Phenotypic nonspecificity is observed with a range of TFs from both within and between TF families and with TFs that recognize distinct DNA-binding sites (Percival-Smith 2017). The wingless and eyeless phenotypes assessed for phenotypic nonspecificity were a result of ectopic expression of TFs. The phenotypes associated with ectopic expression are less straightforward to interpret because the phenotypes are not well characterized, and it is unclear what relevance deletion of a wing or eye has when these phenotypes are not linked to a normal requirement of a TF. Most of the examples of TFs from different families inducing the same phenotype were from the ectopic expression of the TF. The only example of rescue by a TF from a different family is Doublesex male (DSX^M) rescuing the proboscipedia (PB)-dependent growth of the maxillary palp. Rescue of a labial (lab) phenotype by six

Received: January 23, 2023. **Accepted:** March 24, 2023

HOX proteins and rescue of an abdominal-A (abd-A) phenotype by Ultrabithorax (UBX) are unlike rescue of the pb phenotype by DSX^M because the HOX proteins all recognize very similar DNA-binding sites (Greig and Akam 1995; Hirth *et al.* 1998). The rescue of lab and abd-A phenotypes by nonresident HOX proteins can be interpreted in two ways: first, these TFs that recognize similar DNA-binding sites rescue because they recognize similar DNA-binding sites; second, this is an example of phenotypic nonspecificity where multiple TFs, irrespective of the DNA-binding sites recognized, rescue. Therefore, more experiments screening for rescue by TFs that recognize distinct DNA-binding sequences are required to further characterize the properties of phenotypic nonspecificity. The mechanism of rescue is either functional complementation of TFa by TFb or epistatic rescue where the expression of TFb, which is regulated by TFa, functions downstream (epistatic) of TFa rescuing the phenotype. These two possibilities for rescue can be distinguished by showing for functional complementation that the nonresident TF has no role in the phenotype and for epistasis that the nonresident TF is required for the phenotype. Examples of phenotypic nonspecificity are not limited to Drosophila; the three mouse OSK (Oct3/4, Sox2, Klf4) TFs induce pluripotency with very low efficiency that is increased by co-expression of either Myc or Glis1 (Takahashi and Yamanaka 2006; Maekawa *et al.* 2011). In addition, single-cell transcriptomics uncovered phenotypic convergence where distinct sets of TFs regulate the same phenotype in the optic lobe of Drosophila (Konstantinides *et al.* 2018), which is similar to phenotypic nonspecificity where multiple TFs induce or rescue the same phenotype. However, from a technical and conceptual standpoint they are different: phenotypic convergence describes the use of multiple TFs in the determination of the wild-type phenotype; whereas, phenotypic nonspecificity is a nonresident TFb substituting for the resident TFa and requires generating a nonwild-type genotype.

TF function is pleiotropic: a single TF is required for the regulation of multiple genes, and a single TF can be required in multiple tissues/cells for tissue/cell-specific phenotypes; as an example PB is required for the regulation of sets of genes important for the development of either the maxillary palps or the proboscis (Percival-Smith *et al.* 1997). Changes in TF function during evolution are largely attributed to changes in *cis*-regulatory sequences that alter TF expression or expression of TF target genes (Carroll 2008). Because of the autonomous nature of *cis*-regulatory sequences, mutations that affect *cis*-regulatory elements have limited effects. In contrast, due to the constraint and pleiotropy of TFs, protein coding mutations are thought to be deleterious and subject to strong purifying selection. However, these ideas are based on uniform pleiotropy, where each coding mutation affects every trait or function a protein is required for. Differential pleiotropy (the nonuniform effect of mutations) and functional redundancy are two mechanisms that reduce mutational pleiotropy. The multiple differential pleiotropy of alleles observed in genes encoding homeodomain (HD)-containing proteins suggests that the transcription functions of HOX proteins, other than DNA-binding, are dispersed as small redundant protein elements throughout the protein and each of these elements make small, tissue-specific contributions to overall TF function (Hittinger *et al.* 2005; Sivanantharajah and Percival-Smith 2009, 2015). As phenotypic nonspecificity represents functional redundancy of TF function, it is, therefore, appropriate to assess in examples of rescue whether the expression of the nonresident TF exhibits uniform or differential pleiotropy of rescue.

The major questions addressed in this study are as follows: is phenotypic nonspecificity of rescue restricted to a small proportion of *TF* loci?, and is phenotypic nonspecificity rare (1% or less) or more frequent? The *TF* loci chosen for study had reagents available at stock centers and had well-characterized phenotypes. The nonresident TFs were selected by either being the resident TF for one of the other *TF* loci studied or available from a stock center with the UAS insertion expressing a TF on the correct chromosome for the crossing scheme employed. All the TF phenotypes assessed in this study are pleiotropic showing requirement of the TF in multiple phenotypes (Supplementary Table 1). Seven *TF* loci were screened for rescue with at least 12 nonresident TFs. We found phenotypic nonspecificity was frequently observed, the rescue of the phenotypes was differentially pleiotropic, and the rescue was likely due to functional complementation in most cases.

Materials and methods

Drosophila husbandry

Flies were maintained at 23–24 °C and 60% humidity. The flies were reared in 20 mL vials and 300 mL milk bottles containing corn meal media (1% (w/v) Drosophila-grade agar, 6% (w/v) sucrose, 10% (w/v) cornmeal, 1.5% (w/v) yeast, and 0.375% (w/v) 2-methyl hydroxybenzoate). To collect first instar larvae, flies laid eggs on apple juice plates [2.5% (w/v) Drosophila-grade agar, 6% sucrose, 50% apple juice, and 0.3% (w/v) 2-methy hydroxybenzoate], and the progeny aged between 20 and 36 h after egg laying (AEL). All genotypes were assembled using standard Drosophila crosses and crossing schemes. All the Drosophila stocks used in this study are listed in Supplementary Table 2.

Small-scale genetic screens for phenotypic nonspecificity

For the lab, Dfd, Scr, Ubx, fru, and dsx screens, the resident and at least 12 nonresident TFs [Labial (LAB), Deformed (DFD), Antennapedia (ANTP), Sex combs reduced (SCR), Doublesex male (DSX^M), Apterous (AP), Bric a bac 1 (BAB1), Eyeless (EY), Squeeze (SQZ), Forkhead box subgroup O (FOXO), Disconnected (DISCO), Broad Z1(BR.Z1), Broad Z2 (BR.Z2)] were screened for rescue of the six TF phenotypes. All TFs were expressed from UAS constructs inserted on the second chromosome (UASX), and the presence of the correct construct was confirmed with PCR (Supplementary Table 2). The genotypes used in the seven screens of six phenotypes (fru was screened twice) are:

labial screen, *y w; P{UASX, w+} or P{UASX, w+}/CyO; lab^{14}/TM6B, Tb, P{walLy} X y w; P{labGAL4, w+}/CyO; lab^4/TM6B, Tb, P{walLy}*;

Deformed screen, *y w; P{UASX, w+} or P{UASX, w+}/CyO; Dfd^{16}/TM6B, Tb, P{walLy} X y w; P{DfdGAL4, w+}, Ki Dfd^{12}/TM6B, Tb, P{walLy}*;

Sex combs reduced screen, *y w; P{UASX, w+} or P{UASX, w+}/CyO; Scr^4 e/TM6B, Tb, P{walLy} X y w; P{ScrGAL4, w+}/CyO; Scr^2 cu p^p/TM6B, Tb, P{walLy}*;

Ultrabithorax screen, *y w; P{UASX, w+} or P{UASX, w+}/CyO; $Ubx^{abx1,bx3,\ 61d,\ pbx1}$/TM6B, Tb, P{walLy} X y w; $Ubx^{6.22}$, P{UbxGAL4, w+}/TM6B, Tb, P{walLy}*;

fruitless screens, *y w; P{UASX, w+} or P{UASX, w+}/CyO; fru^{4-40}/TM6B, Tb, P{walLy} X y w; fruGAL4A or fruGAL4B/TM6B, Tb, P{walLy}*;

doublesex screen, *y w; P{UASX, w+} or P{UASX, w+}/CyO; dsx^1/TM6B, Tb, P{walLy} X w; dsxGAL4/TM6B, Tb*.

Two control stocks for the Ubx and dsx screens with UAS insertions on the third chromosome are: *y w; P{UASUbx, w+}, $Ubx^{abx1,bx3,\ 61d,\ pbx1}$/TM6B, Tb, P{walLy}*, and *y w; P{UASdsx^F, w+}, dsx^1/TM6B, Tb, P{walLy}*, respectively.

Large-scale screens for phenotypic nonspecificity

For large-scale screens, greater than 50 nonresident TFs were screened. To screen for sex-specific changes in abdominal pigmentation, *P{UASX, w+}* were crossed with *y w/Dp(1: Y) B^{s}; dsxGAL4/TM6B, P{walLy}*. Bar eyed progeny (XY) were screened for female abdominal pigmentation, and nonbar eyed progeny (XX) were screened for male abdominal pigmentation. For subsequent characterization of the phenotypes, *w; dsxGAL4/TM6B* were crossed with *P{UASX, w+}* and the chromosomal sex of the progeny was assessed by the effect that dosage compensation has on the w^{+} phenotype (XY eyes are darker than XX eyes).

For the screen for rescue of apterous (ap), insertions of *UASX* on the third chromosome were used. The final cross of the screen was either (1) *apGAL4/CyO X w; ap^{DG3}/L; P{UASX, w+}/TM6B, Tb, P{walLy}* or (2) *y w; apGAL4/CyO; P{GAL80^{ts}, w+} X y w; ap$^{MIO1996\text{-}FLPSTOP.D}$/L; P{UASX, w+}/TM6B, P{walLy}*. The progeny of the second screen were transferred to 29 °C between 24 and 72 h AEL to activate GAL4 activity by inactivating GAL80 activity and were kept at 29 °C until late pupation/eclosion.

Analysis of the epistatic interactions between the expression of ANTP, EY, or HB and *bab*

For the expression of DSX^{M}, BAB1, ANTP, EY, and HB in a *bab1 dsx^{1}* mutant background, *y w; P{UASX, w+}; Df (3L)bab1^{Fpa2} dsx^{1}/TM6B, Tb, P{walLy} X w; Df(3L)bab^{Ar07} dsxGAL4/TM6B, Tb*. For expression of DSX^{F} in a *bab1 dsx^{1}* mutant background, *y w; Df(3L)bab1^{Fpa2} dsx^{1}, P{UASdsx^{F}, w+}/TM6B, Tb, P{walLy} X w; Df(3L)bab^{Ar07} dsxGAL4/TM6B*, Tb. Nontubby, nonhumeral progeny of the crosses were collected, and images recorded.

RNAi knockdown of expression

RNAi stocks were obtained from Bloomington Drosophila stock center and crossed with either *w; rnGAL4, y w; Ubx$^{6.22}$, P{UbxGAL4, w+}/TM6B, Tb, P{walLy}, y w; fruGAL4A* or *fruGAL4B/TM6B, Tb, P{walLy}, w; dsxGAL4/TM6B, Tb* or *y w; apGAL4/CyO; Ki ftz^{11}/TM6B, Tb, P{walLy}*.

Phenotypic analysis

For the lab, Dfd, and Scr screens, the *Hox^{null}* genotypes are marked independently of the Hox phenotype with yellow. In all crosses, the parents share the basic genotype *y; Hox^{null}/TM6B, Tb, P{walLy}*, and therefore, the *y; Hox^{null}/Hox^{null}* progeny are y because all other genotypes carry *TM6B, Tb, P{walLy}*, which are y^{+} (Hyduk and Percival-Smith 1996). At 20–32 h AEL, first instar larvae were dechorionated with bleach and devitellinized by shaking in a 1:1 heptane:methanol mixture. The larvae were mounted in Hoyer's mountant and viewed under bright field, phase contrast or dark field optics (Wieschaus and Nusslein-Volhard 1986). The bright field images of the head skeletons were processed with an extended focus program of the software Zen (Zeiss, Oberkochen, Germany). The phase contrast images were processed with the software ImageJ (NIH, Bethesda, USA). The proportion of *Hox^{null}* embryos hatched relative to the number of eggs laid was determined. For labial morphometric analysis, the distance between mouthhooks and the length of the head skeleton were measured using Open lab software (Leica, Wetzlar, Germany). To count the number of sex combs in the Scr screen, the first legs of *y w; P{ScrGAL4, w+}/P{UASX, w+}; Scr^{4} e/TM6B, Tb, P{walLy}* were collected and mounted in Hoyer's mountant.

For the Ubx screen, the *y w; P{UASX, w+}/+; Ubx$^{abx,bx,\ 61d,\ pbx}$/Ubx$^{6.22}$, P{UbxGAL4, w+}* genotypes were identified as adults or pupae by their nonhumeral or nontubby phenotypes, respectively (lacking *TM6B, Tb, P{walLy}*). Eclosed or pharate adults of the correct genotype were critical point dried, sputter coated and imaged with scanning electron microscopy (SEM) at the Biotron Integrated Microscopy Laboratory or at Surface Science Western (London, ON).

For all assays of the fru screen, freshly eclosed male flies were placed in separate vials and aged for 3–5 days (Villella *et al.* 1997). For the fertility assay, individual males were mated with two wild-type 2-day-old virgin females and the females allowed to lay eggs for 3 days and the vials were inspected for larvae at 7 days after mating. For the courtship assays, males were introduced to either 2-day-old virgin females or 2-day-old males (marked on the wings with a Sharpie marker), and their behavior recorded for 10 min on a video. The videos were scored for orienting, male follows female/male, male wing extension, genital licking, attempted copulation, and copulation behaviors associated with male mating activity and a courtship index (CI) determined.

To count and image sex combs for the dsx screens, the first pair of legs were mounted in Hoyer's mountant. The dorsal abdomens were imaged with a dissecting microscope and the images processed with the extended focus function of the software Zen. To image the genitals, eclosed flies were critical point dried, sputter coated, and imaged with SEM. The ap phenotypes were recorded as SEM images of eclosed adult flies.

Statistical analysis

When an ordinary ANOVA was performed, the data (untransformed or transformed) was assessed as being normally distributed and of equal variance with QQ plots and plotting residuals. In some analyses of sex comb number for dsx experiments, the zero data was ignored when considering whether the criteria for an ordinary ANOVA was met. For the lab head skeleton lengths and Scr, or dsx, number of sex combs data, an ordinary ANOVA was performed and followed with a Tukey's or Dunnett's post hoc analysis. For the number of sex combs induced with *rnGAL4*, the data was log transformed to meet the criteria of an ordinary ANOVA and followed with a Tukey's post hoc analysis. The CI indexes of M/F and M/M courtship were transformed with arcsin and log(arcsin), respectively, to meet the criteria of an ordinary ANOVA. For the rescue of lab, Dfd, Scr, fru (male fertility), and the number of sex combs of male *dsxGAL4* flies expressing different TFs, an ANOVA of ranks was performed followed by a Dunn's post hoc analysis. To assess the similarities of expected and observed for the rescue of lab, Dfd and Scr, Chi-squared tests were performed. The analyses were performed in the software package Prism (Graphpad).

Results

Overview of screens for phenotypic nonspecificity

Phenotypic nonspecificity is observed with ectopic expression of both HOX and non-HOX TFs (Percival-Smith 2017); however, the only example of rescue with a non-HOX TF is the rescue of the pb maxillary palp phenotype by DSX^{M}. Rescue of a phenotype has a more straight-forward interpretation than the induction of a phenotype by ectopic expression, and also the rescue of pleiotropic phenotypes allows the assessment of differential/uniform pleiotropy (Supplementary Table 1). We used the *UAS/GAL4* system to assess the phenotypic rescue of seven TF phenotypes by the expression of at least 12 nonresident TFs. For the four *Hox* loci (*lab*, *Dfd*, *Scr*, *Ubx*), we used drivers composed of *Hox* regulatory elements fused to GAL4 (Jenett *et al.* 2012). Genetic backgrounds were created that carried the driver and were hemizygous for

null *Hox* alleles. For dsx, fru, and ap, we used driver stocks with insertions of *GAL4* into the *TF* loci that created both a loss-of-function allele for these loci and expressed GAL4 from the regulatory sequences of these loci. In these genetic backgrounds, we screened for rescue of the phenotype by resident and nonresident TFs expressed from *P{UASTF}* insertions.

Labial

Drosophila lab^4/lab^{14} larvae lacked the H-piece, including the bridge and the lateral bar (Figs. 1, a1 and 2d) (Diederich *et al.* 1989; Merrill *et al.* 1989). Furthermore, the two mouth hooks were widely separated in the mutant, relative to the wild type, due to failure of head involution (Figs. 1, a1 and 2d). Since both the *labGAL4* and *UAS-lab* insertions were heterozygous, the expected frequency of embryonic rescue among the yellow cuticles was 25%. Of the 50 yellow cuticles (lab^4/lab^{14}) examined in experiments assaying LAB expression, 11 were rescued (Figs. 1, a2 and 2b). This was similar to the expected 12.5 [χ^2 (1, 50) = 0.18, P = 0.7]. The expression of LAB from *UAS-lab* rescued embryonic head involution and head skeleton defects (H-piece lateral bar, the dorsal bridge, and H-piece bridge) (Figs. 1, a2 and 2b). Out of 238 hatched larvae examined, 8 larvae were yellow; however, none of these larvae survived to the third instar larval/pupal stage. No examples of pupal (non-Tb)/adult rescue were observed when progeny were allowed to develop to adulthood.

The expression of 12 nonresident TFs were screened for rescue by carefully examining 50 yellow cuticles, and rescue in 9 larval cuticles expressing DSX^M were identified (Fig. 1, a11). This frequency of rescue was similar to the expected 12.5 [χ^2 (1, 50) = 0.98, P = 0.3]. One y larva expressing DSX^M of the 172 larvae hatched was found but did not survive to the third instar larval/pupal stage. No examples of pupal (non-Tb)/adult rescue were observed when progeny were allowed to develop to adulthood.

The rescues with LAB and DSX^M were differentially pleiotropic. First, LAB rescued the head involution phenotype such that the mouth hooks were in close proximity and rescued development of the H-piece lateral bar and dorsal bridge, and DSX^M only rescued the mouth hooks phenotype (Fig. 2, b and c). Second, with morphometric analysis measuring the distance between the two tips of the mouth hooks and the distance between the anterior end of the head and the posterior end of ventral arms of the head skeleton (head length) (Fig. 2, a–d), clear differences between the rescued and mutant larvae (Fig. 2, e and f) in both mouth hook distance and head length were observed. The rescue of head involution (mouth hook distance) was very strong with expression of either LAB or DSX^M suggesting it could be used as a marker of the second chromosome genotype (*UAS-lab/labGAL4* or *UAS-*dsx^M*/labGAL4*) for the analysis of the rescue of head length (Fig. 2e). Both LAB and DSX^M rescued head length, relative to the *lab* null mutant, but the rescues with LAB and DSX^M were differentially pleiotropic and distinct from the full rescue of mouth hook distance with both LAB and DSX^M, as the rescue with LAB was not wild type ($P < 0.0001$) and was stronger than observed with DSX^M ($P < 0.0001$) (Fig. 2f). The head skeleton of *dsxGAL4/*dsx^1 viable larvae are wild type, indicating that DSX^M is not required for larval head skeleton development and is not a candidate for a TF that functions downstream of LAB (Supplementary Fig. S1b).

Deformed

DFD deficient (Dfd^{12}/Dfd^{16}) larvae lacked the mouth hooks (Fig. 1, b1) and cirri (Regulski *et al.* 1987; Zeng *et al.* 1994). Because the third chromosome carried both the *Dfd GAL4* insertion and the Dfd^{12} null allele and the *UAS-Dfd* insertion was heterozygous on the second chromosome, the expected maximum frequency of rescue was 50%. Of the 50 yellow cuticles (Dfd^{12}/Dfd^{16}) examined assessing DFD rescue, 13 had one or two mouth hooks (Fig. 1 b3)

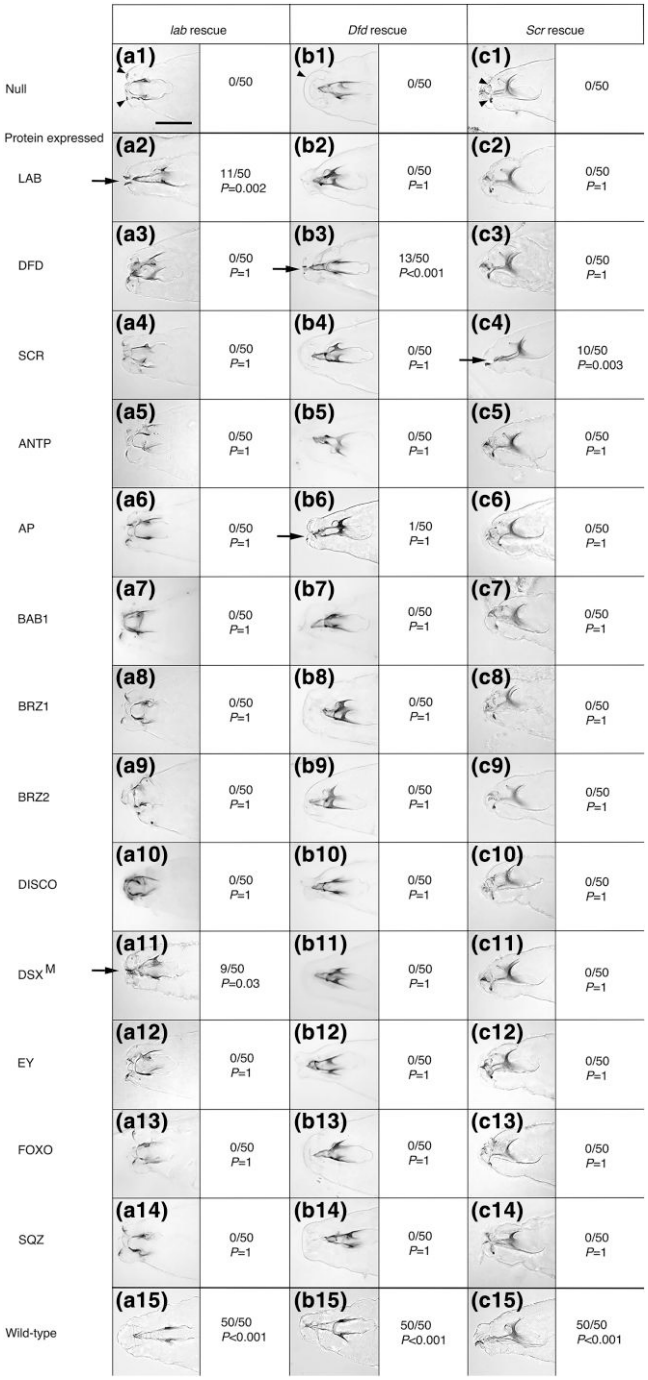

Fig. 1. Screens for the rescue of lab a), Dfd b), and Scr c) phenotypes. All panels are brightfield images of the head skeleton. The lab^{null} genotype is lab^4/lab^{14}; the Dfd^{null} genotype is Dfd^{12}/Dfd^{16}; and the Scr^{null} genotype is Scr^2/Scr^4. For all assays of rescue, 50 y larvae were examined, and the frequency of rescue indicated in the column to the right for lab and Scr. For Dfd, the number of rescued mouth hooks was assessed. The rescue data was analyzed using an ANOVA on ranks [lab H (14) = 561, $P < 0.0001$; Dfd H (14) = 624, $P < 0.0001$; Scr H (14) = 640, $P < 0.0001$]. The P values of a Dunn's post hoc test relative to the control null mutant are indicated below the frequency of the rescue. The nonresident TF expressed are indicated on the left. The scale bar in a1 indicates 100 μm and is the same in all other images. The arrows indicate rescue of lab, Dfd, and Scr phenotypes.

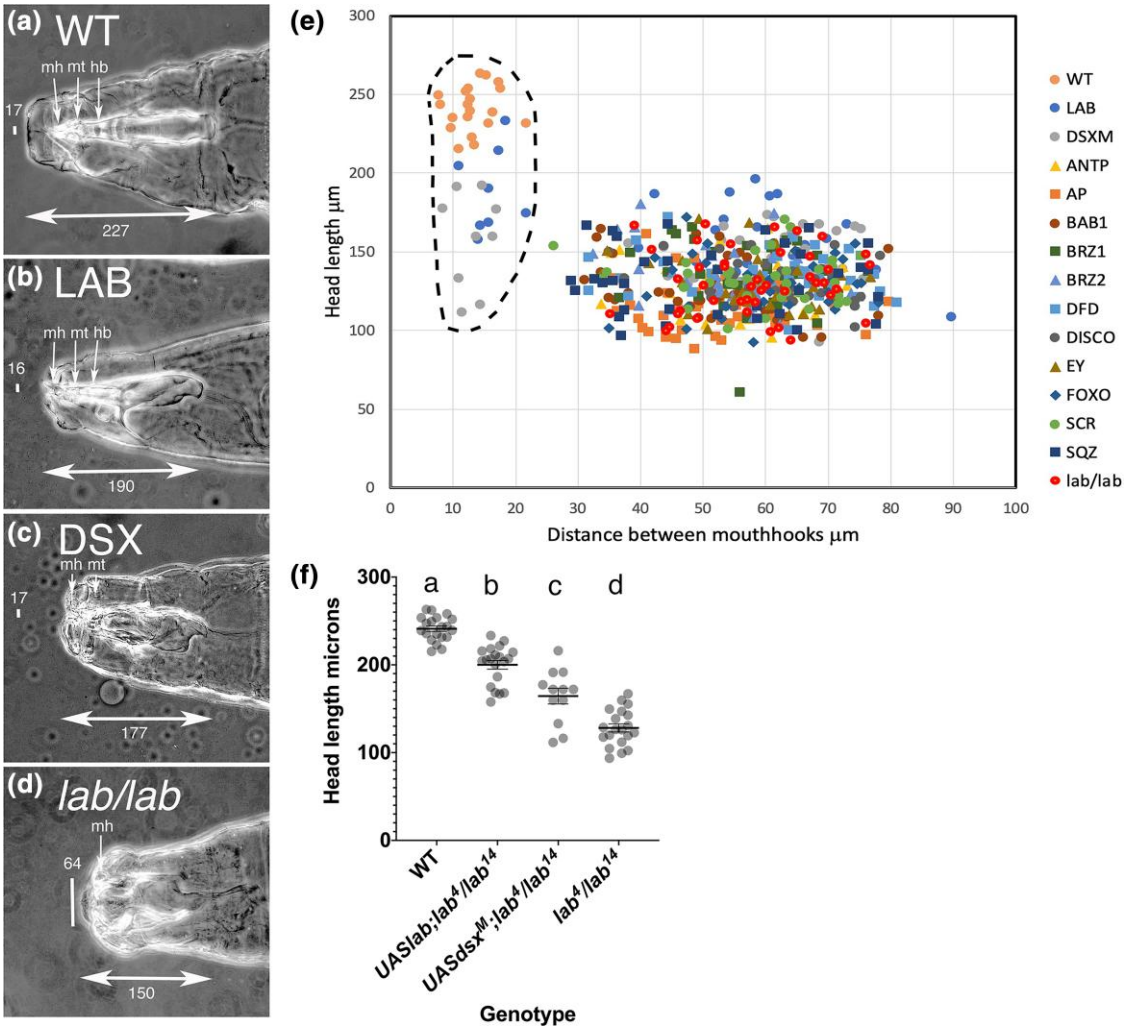

Fig. 2. Characterization of the rescue of the lab phenotype. Panels (a)–(d) are phase contrast images of the larval head skeleton. Panel (a) is wild-type (*y w*); panel b is *y w; UAS-lab/labGAL4; lab*^{14}*/lab*^{4}; panel (c) is *y w; UAS-dsx*^{M}*/labGAL4; lab*^{14}*/lab*^{4}; and panel (d) is *y w; lab*^{14}*/lab*^{4}. The vertical line is the measurement (µm) between mouth hooks and the horizontal line is the measurement of the length of the head skeleton (head length). The arrows indicate mh: mouth hooks; mt: medium teeth; hb: H-piece bridge. Panel (e) is a plot of the distance between mouth hooks vs head length for all larvae. The dotted line encompasses larvae with a short distance between mouth hooks and an increased head length. Panel (f) is a scatter plot of head length of the head skeleton of the rescued larvae, wild type and *lab*^{null} mutant. An ordinary ANOVA was performed ($F_{3, 68} = 98$, $P < 0.0001$) followed by a Tukey's pair-wise comparison; the same letter indicates no difference ($P > 0.05$). The mean and SEM are indicated.

and 3 had cirri. This was less frequent than the 25 expected for strong rescue [χ^2 (1, 50) = 5.76, $P = 0.02$]. Of the 248 hatched larvae examined, one yellow larva was found but the larva did not survive to the late third instar larval/pupal stage. No examples of pupal (non-Tb)/adult rescue were observed when progeny were allowed to develop to adulthood. The expression of 12 nonresident TFs were screened for rescue by carefully examining 50 yellow cuticles for each TF expressed. Although one larva expressing AP exhibited rescue of a mouth hook, the frequency of rescue was too low to be considered significant (Fig. 1, b6).

Sex combs reduced

During embryogenesis and metamorphosis, SCR is required for head and thorax development (Sivanantharajah and Percival-Smith 2009). *Scr*^{2}*/Scr*^{4} larvae are missing the medium tooth, and the anterior portion of the H-piece structure is curved toward the ventral side (Fig. 1, c1). Because both the *ScrGAL4* and *UAS-Scr* insertions were heterozygous, the expected maximum frequency of embryonic rescue is 25%. Of the 50 yellow larvae (*Scr*^{2}*/Scr*^{4}) examined assessing SCR expression, 10 were rescued (Fig. 1, c4), which was similar to the expected 12.5 (χ^2 (1, 50) = 0.5, $P = 0.5$). Of the 162 hatched larvae examined, no yellow larvae hatched, and no non-Tb pupae were observed when progeny were allowed to develop to adulthood. Head skeleton defects (Fig. 1, c4) and T1 beard formation (Fig. 3, a–c) were rescued with the expression of SCR. The number of setae in the T1 beard in larvae with rescue of the head skeleton (*ScrGAL4/UAS-Scr*) was rescued ($P < 0.0001$); however, the number of setae in the T1 beard of these rescues was less than that observed in wild-type controls ($P < 0.0001$). In addition, expression of SCR was found to increase the number of male sex combs by about two bristles in a *Scr*^{4}*/Scr*$^{+}$ heterozygote (Fig. 3e; $P < 0.0001$). The number of sex combs is linearly associated with the dose/activity of SCR (Sivanantharajah and Percival-Smith 2009); therefore, the increase of two bristles suggests that the expression of SCR from *UAS-Scr* by *ScrGAL4* is 20% of wild-type levels. Both the T1 beard and sex comb data suggest that the level of SCR expression using the *ScrGAL4* driver and *UAS-Scr* was less than wild-type levels.

The expression of 12 nonresident TFs were screened for rescue by carefully examining 50 yellow cuticles for each TF. No rescue of

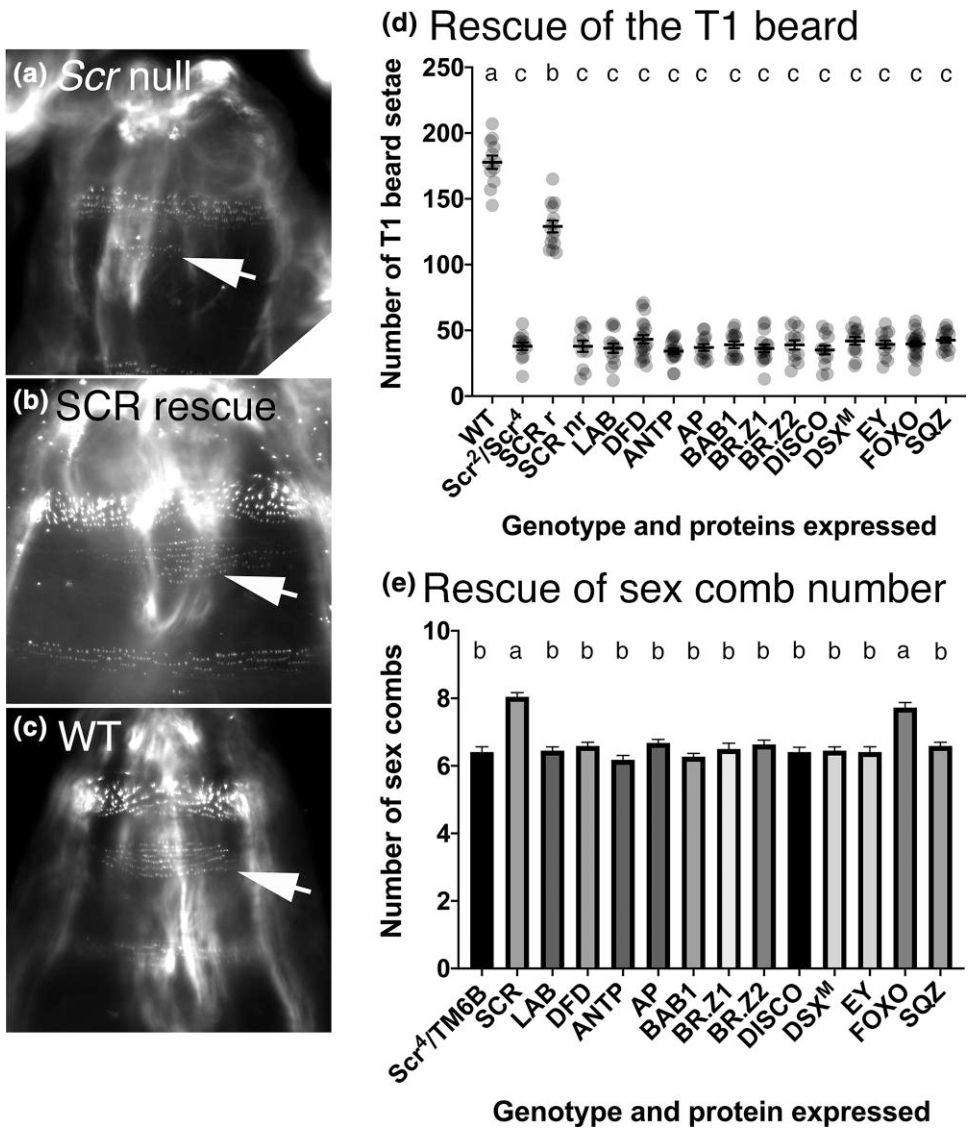

Fig. 3. Screens for the rescue of the Scr phenotypes. Panels (a)–(c) are dark field micrographs of larval T1 segments. The arrows point to T1 beards of a Scr^2/Scr^4 larva (a), a *ScrGAL4/UAS-Scr*; Scr^2/Scr^4 larva (b) and a wild-type larva (c). Panel (d) is a scatter plot of the number of T1 setae in various genotypes. SCRr and SCRnr refers to the number of setae on larval cuticles that have rescued head skeletons (r) and the number of setae on larval cuticles that exhibit no rescue (nr), respectively. Analysis of the data with an ordinary ANOVA ($F_{15,\ 212} = 148$; $P < 0.0001$) detected differences, and data that are not different ($P > 0.05$) have the same letter using Tukey's post hoc pair-wise comparisons. Panel (e) is a bar graph of the number of sex combs on *ScrGAL4*; $Scr^4/+$ male adults expressing no protein or the indicated protein. An ordinary ANOVA detected differences ($F_{13,\ 294} = 17$, $P < 0.0001$) and the pair-wise comparisons using Tukey's post hoc analysis that were not different are indicated with the same letter ($P > 0.05$). The mean and SEM are indicated in panels (d) and (e).

the head skeleton defects was observed. The number of T1 beard setae were counted on at least 12 yellow larvae for each TF and no rescue of beard formation was observed (not a single larva had more than 80 setae) (Fig. 3d). The number of sex combs were counted on *P{UAS-TF}/P{ScrGAL4}*; $Scr^4/TM6B$ adult males. The expression of FOXO increased the number of sex combs by about two bristles ($P < 0.0001$) (Fig. 3e). The rescues with SCR and FOXO were differentially pleiotropic, as the expression of SCR rescued larval head skeleton, T1 beard formation and increased the number of sex combs, whereas the expression of FOXO only increased the number of sex combs.

To test whether expression of FOXO induces ectopic sex combs like SCR, *rnGAL4* was used to drive *UAS-Scr* and *UAS-foxo* expression in all three pairs of legs of male flies (Fig. 4) (Sivanantharajah and Percival-Smith 2014). The number of sex combs on the first leg was increased relative to the wild-type by the presence of *rnGAL4* ($P = 0.0001$) (Fig. 4j). Ectopic expression of SCR increased the number of sex combs on the first leg (Fig. 4d) and induced ectopic sex combs on the second and third legs (Fig. 4, e and f). Ectopic expression of FOXO increased the number of sex combs by two bristles on the first leg from 11.4 (*rnGAL4*) to 13.3 ($P = 0.04$) (Fig. 4, g and j) but did not induce ectopic sex combs on the second and third legs (Fig. 4, h and i). This is an additional example of the differential pleiotropy of SCR and FOXO: SCR increases the number of sex combs and induces ectopic sex combs but FOXO only increases the number of sex combs.

To test whether expression of FOXO is required for sex combs development, and therefore, a candidate for regulating, or being regulated by, SCR, two *FOXO* RNAi molecules (*TRiP.HMS00793* and *TRiP.JF02734*; Perkins *et al.* 2015) were expressed with *rnGAL4*. In neither case was a decrease in the number of first leg sex combs relative to the *rnGAL4* control observed ($P = 0.5$, 0.6);

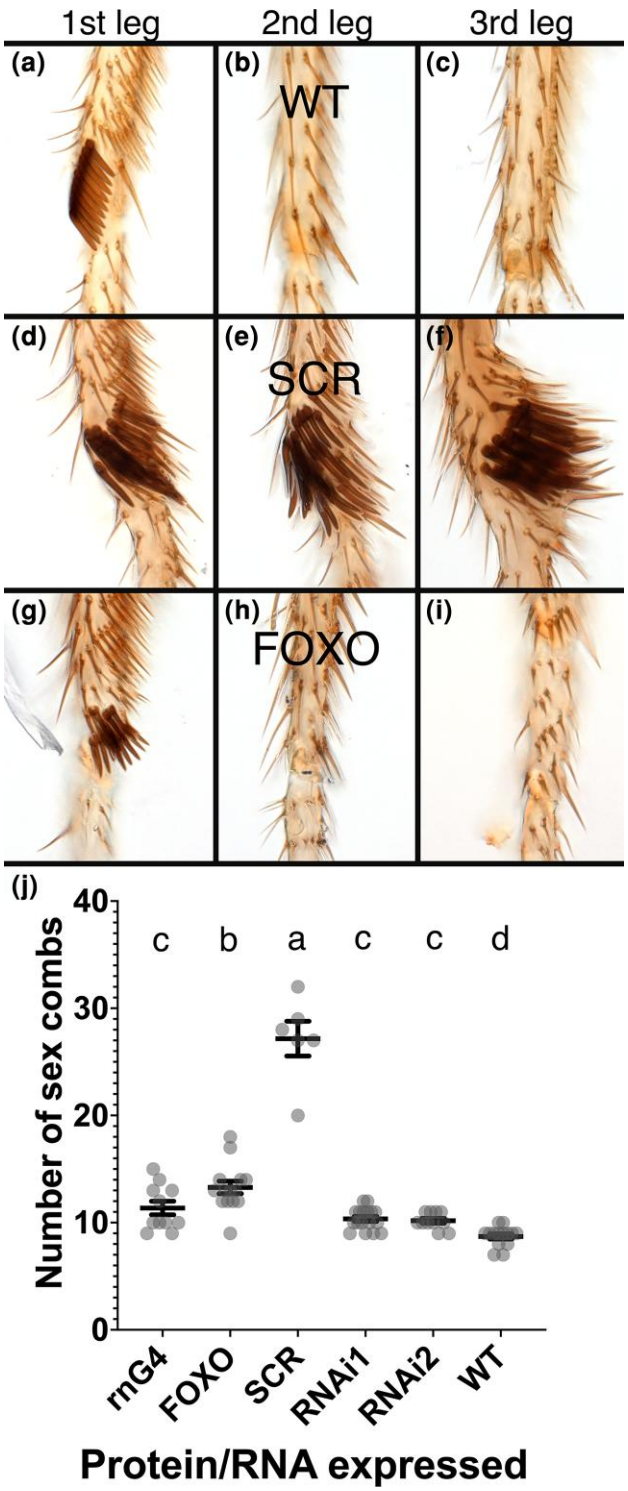

Fig. 4. The phenotype of ectopic expression of SCR and FOXO in male legs and the nonrequirement of FOXO for sex combs formation. The *rnGAL4* driver was used to ectopically express SCR, FOXO, and two *FOXO* RNAi molecules in male legs. Panels (a)–(c) are wild-type legs. Panels (d)–(f) are the effects of ectopic expression of SCR in the first, second, and third male leg, respectively. Panels (g)–(i) are the effects of ectopic expression of FOXO in the first, second, and third male leg, respectively. Panel (j) are scatter plots of the number of sex combs on the first leg of male flies that have the *rnGAL4* driver alone, with *UAS-Scr*, *UAS-foxo*, *P{UAS-TRiP.HMS00793}* (RNAi1), *P{UAS-TRiP.JF02734}* (RNAi2), and a wild-type control. An ordinary ANOVA detected differences ($F_{5,\ 67} = 69$, $P < 0.0001$) and the pair-wise comparisons using Tukey's post hoc analysis that were not different are indicated with the same letter ($P > 0.05$). The mean and SEM are indicated.

therefore, these experiments provide no evidence for a requirement of FOXO in determining the number of sex combs that normally form (Fig. 4j).

Ultrabithorax

Taking genomic DNA fragments from the *Ubx* locus and screening them for enhancer activity when fused to *GAL4* identified a fragment that reproduced the UBX embryonic expression pattern. This driver is expressed throughout the haltere imaginal disc and is expressed ectopically in the notum and wing pouch of the wing imaginal disc (Jenett *et al.* 2012). The third chromosome carrying the *UbxGAL4* insertion also carried a y^+ allele; therefore, rescue of the Ubx larval cuticular phenotype could not be assessed. The genotype $Ubx^{abx1\ bx3\ 61d\ pbx1}/Ubx^{9.22}$ *P{UbxGAL4, w⁺}* was used to assess rescue of the adult viable $Ubx^{abx1\ bx3\ 61d\ pbx1}$ hypomorphic allele. This allelic combination gives the classic four-winged fly (Weinzierl *et al.* 1987; Rivlin *et al.* 2001), where the third thoracic segment (T3) with its haltere are transformed into the likeness of the second thoracic segment (T2) (Fig. 5, b and c). Expression of UBX in this mutant background resulted in partial rescue of the haltere to wing transformation in T3; the scabellum and pedicellum were wild-type in appearance (of particular note are the transverse rows of fused type 5 campaniform sensilla specific to the haltere) (Fig. 5, d, e, and f) (Cole and Palka 1982). Although the wing in T3 was drastically reduced, the capitellum was not rescued (the capitellum has characteristic short trichomes) (Fig. 5, e and f). In addition, expression of UBX in T3 suppressed the T2-like notum such that it has a wild-type appearance (Fig. 5d). The ectopic expression of UBX in the wing imaginal disc due to ectopic expression of GAL4 in the developing wing from *UbxGAL4* resulted in a reduction of the wing and partial transformation to a haltere and partial suppression of the T2 notum (Fig. 5d). The partial transformation of the wing to a haltere included transformation of unfused, wing campaniform sensilla on the dorsal proximal radius to fused type 5, haltere-like sensilla (Figs. 5, g, h and 6, d, e). In addition, 2/15 flies lacked the third legs; 7/15 lacked one third leg, and the remainder had six legs which is the opposite of an extra leg on the first abdominal segment observed with hypomorphic *Ubx* alleles (Lewis 1963) suggesting that the loss of the third leg is due to a gain of UBX function.

Thirteen nonresident TFs were screened for an effect on the Ubx hypomorphic phenotype. Expression of DFD was either embryonic or larval lethal, and the expression of BR.Z1, BR.Z2, and FOXO in $Ubx^{abx1\ bx3\ 61d\ pbx1}/Ubx^{9.22}$ *P{UbxGAL4, w⁺}* flies caused failure to develop to pharate or eclosed adults during metamorphosis. The eclosed adults that expressed DISCO and BAB1 had four wings (Fig. 5, i and j). Flies expressing AP, and SQZ did not eclose, but the pharate adults had the four-winged phenotype (Fig. 5, k and m). Flies expressing DSX^M did not eclose but the pharate adults still had the four-winged phenotype and an extensive deletion of the notum in T2 and T3 (Fig. 5l). Flies expressing LAB eclosed with the four wings transformed into tissue with micro and macrochaetes (Fig. 5, p and t). Flies expressing SCR did not eclose and only had two wings plus a reduction of the T2 notum (Fig. 5, q and u). The two-winged phenotype was not due to the rescue of T3 to wild type with a haltere but was a deletion of the derivatives of the haltere imaginal disc (Fig. 5u). Flies expressing ANTP and EY did not eclose and the four wings were reduced (Fig. 5, n and o). The reduced wings on T2 and T3 of ANTP expressing flies had fused type 5 campaniform sensilla characteristic of a haltere indicating a transformation toward haltere identity (Figs. 5r and 6, e and f). T3 expressing ANTP was not rescued to wild type and some of the notum of T2 was absent.

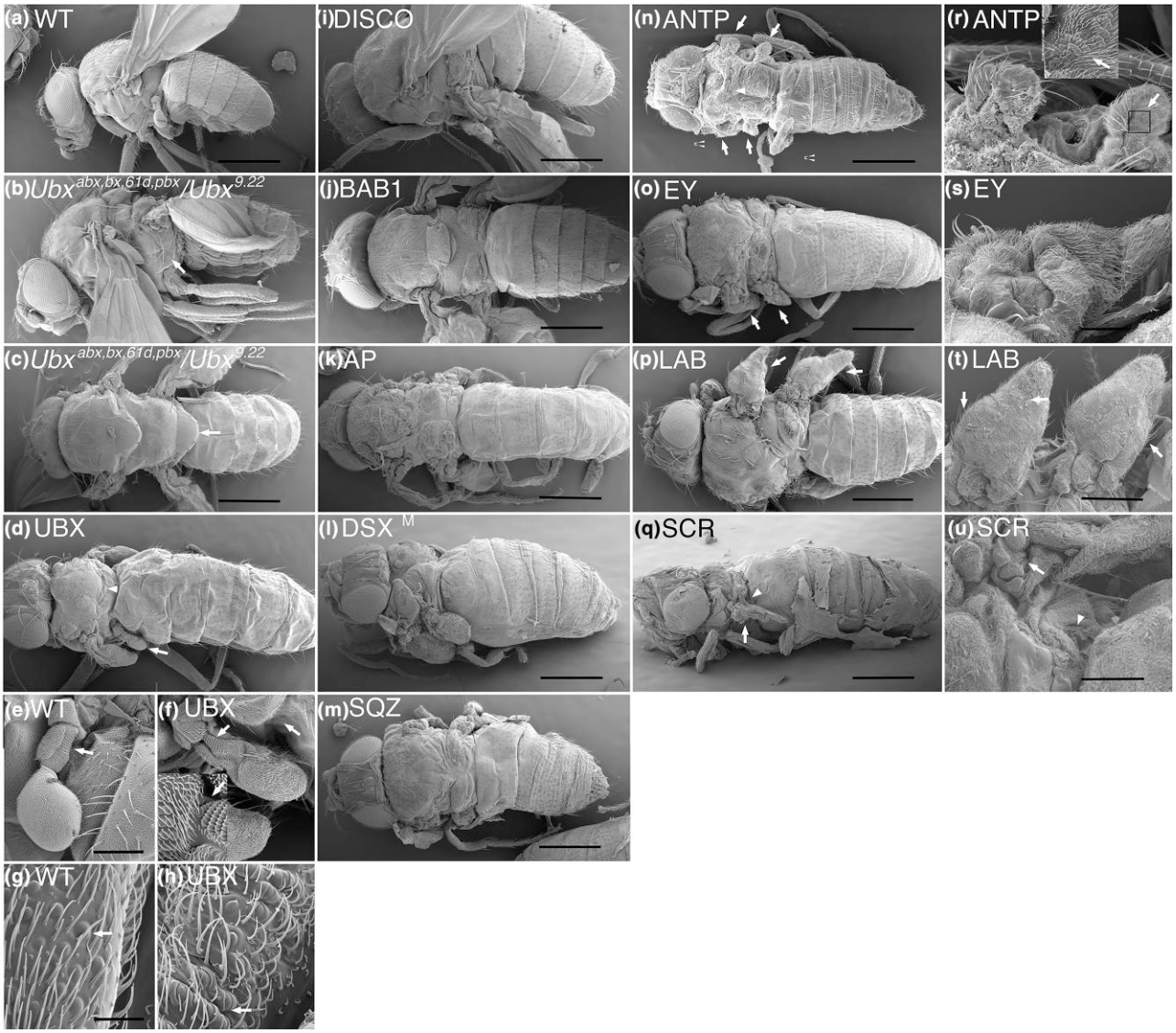

Fig. 5. Screen for rescue of adult Ubx phenotypes. In all panels either the genotype or proteins expressed in a $Ubx^{abx1\ bx3\ 61d\ pbx1}/Ubx^{9.22}$ background are indicated in the top left-hand corner. (a) wild-type fly. Panels (b) and (c) are lateral and dorsal images of $Ubx^{abx1\ bx3\ 61d\ pbx1}/Ubx^{9.22}$ flies. Panel b the second additional pair of wings indicate a T3 to T2 transformation (arrow). Panel c the arrow points to transformation of T3 to T2. Panels d, f, h are the expression of UBX in $Ubx^{abx1\ bx3\ 61d\ pbx1}/Ubx^{9.22}$ flies. In Panel d the wings are reduced (arrow), T3 is rescued and some of T2 notum development is suppressed (arrowhead). (e), The arrow indicates the scabellum and pedicellum with the associated campaniform sensilla of a wild-type fly. In panel (f), the scabellum and pedicellum (arrow) are restored by expression of UBX indicating rescue of the haltere development (arrows), and the insert is a close up of the haltere specific transverse rows of fused type 5 campaniform sensilla. In panel (g) is the campaniform sensilla of a wild-type T2 wing (arrow). (h), The fused haltere-like sensilla (arrows) indicate a wing to haltere transformation due to ectopic UBX expression in the developing T2 wing. Panels (i) and (j) are eclosed adults expressing DISCO and BAB1, respectively. Panels (l)–(m) are pharate adults expressing AP, DSX^{M}, and SQZ, respectively. Panels (n)–(q) are pharate adults expressing ANTP, EY, LAB, and SCR, respectively. Panels (r)–(u) are close ups of T2 and T3 of pharate adults expressing ANTP, EY, LAB, and SCR, respectively. In panel (n), the wings on T2 and T3 are reduced (arrows) and some of the notum of T2 is absent (arrowhead). In panel (r), the fused type 5 campaniform sensilla characteristic of a haltere indicate rescue toward a haltere (arrows). The insert in panel r is a close up of the haltere-like fused type 5 campaniform sensilla. In panel (o), the wings are reduced (arrows). In panel (s), the wing is reduced. In panels (p) and (t), the four wings are transformed into tissue with micro and macrochaetes (arrows). In panels (q) and (u), the remaining wing is indicated with an arrow, and the region where normally a haltere develops is indicated with an arrowhead. The bars in panels (a)–(d), (i) and (j)–(q) indicate 500 μm; the bars in panels (r), (t), and (u) indicate 200 μm; the bars in panels (e), (f), and (s) indicate 50 μm; the bars in panels (g) and (h) indicate 10 μm.

The rescue with UBX, EY, and ANTP were differentially pleiotropic. UBX, EY, and ANTP reduced the wings but only the wings expressing UBX and ANTP had fused type 5 campaniform sensilla that are haltere-like. In addition, only UBX rescues the T3 notum to wild type.

To test whether ANTP is required for development of the haltere, *ANTP*RNAi molecules from *P{UAS-TRiP.JF02754}* (Fig. 6h) and *P{UAS-TRiP.HMC05799}* (Supplementary Fig. S1c) where expressed with *UbxGAL4* (Fig. 6g). Both *ANTP*RNAi molecules had no effect on the development of the halteres and specifically the development of fused type 5 campaniform sensilla. This lack of an effect with RNAi along with lack of a recorded effect in other studies of ANTP function (Struhl 1981; Abbott and Kaufman 1986) suggests that ANTP is not required for haltere development.

Fruitless

The *fru* locus is a structurally complex gene that expresses multiple protein isoforms (Anand *et al.* 2001). Of the many protein

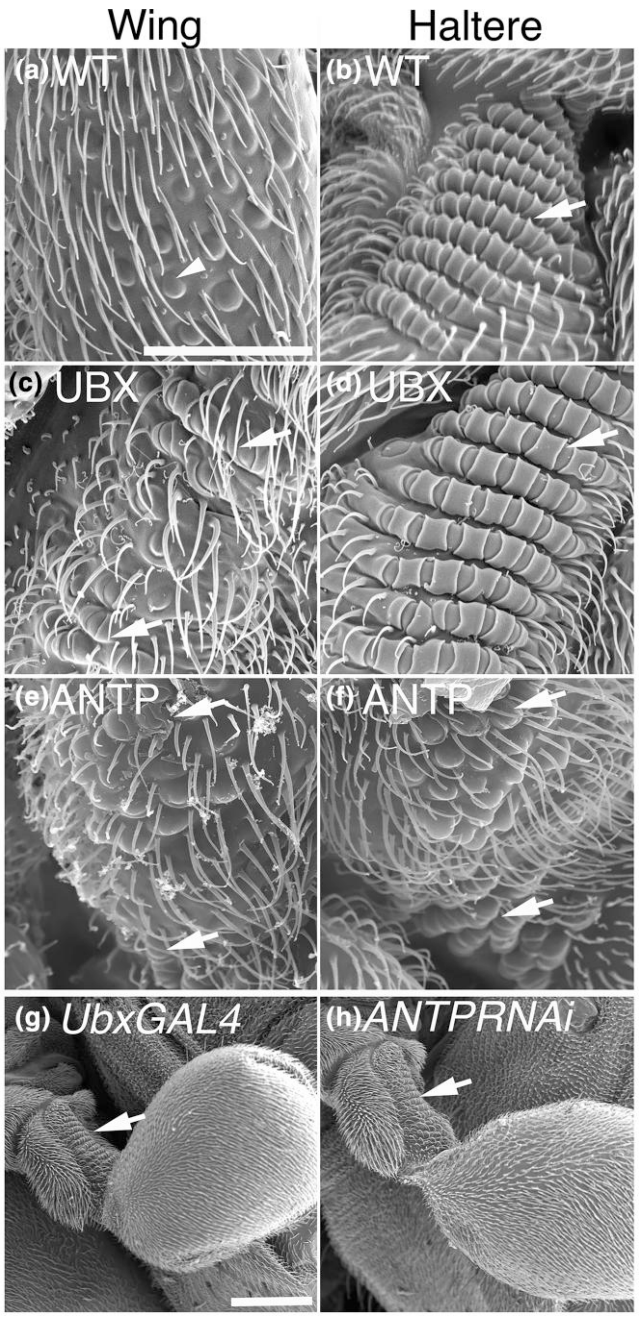

Fig. 6. Rescue of fused type 5 campaniform sensilla by UBX and ANTP, and the effect of expression of *ANTP*RNAi. At the top left of panels a–f, wild type or the protein expressed in a $Ubx^{abx1\ bx3\ 61d\ pbx1}/Ubx^{9.22}$ background are indicated. Panels (a) and (b) are a wild-type wing and haltere, respectively, showing the type 4 campaniform sensilla (circular low profile without a socket) typically found on the wing proximal radius (arrowhead) and the transverse rows of fused type 5 campaniform sensilla found on the dorsal pedicellum (arrow) (Cole and Palka 1982). Panels (c) and (d) express UBX. In the wing proximal radius fused type 5 sensilla are present (arrows) and the dorsal pedicellum is rescued with the transverse rows of fused type 5 campaniform sensilla. Panels (e) and (f) express ANTP. In both the wing and haltere fused type 5 sensilla are present indicating a transformation toward haltere identity (arrows). The bar in panel (a) indicates 20 μm for panels a–f. Panel g is an image of control *UbxGAL4*, $Ubx^{6.22}$/+ flies and panel (g) is an image of *UbxGAL4*, $Ubx^{6.22}$/*P{UAS-TRiP.JF02754}* which expresses an *ANTP*RNAi molecule. The arrows indicate fused type 5 sensilla of the ventral pedicellum in both panels (g) and (h). The scale bar in panel (g) indicates 50 μm for both panels (g) and (h).

isoforms expressed, those translated from transcripts initiated at the *P1* promoter and spliced in a male-specific pattern are required for male fertility and courtship (Demir and Dickson 2005). Expression of the three major FRU^M isoforms are required for male courtship behavior (Neville *et al.* 2014; von Philipsborn *et al.* 2014). Phenotypic nonspecificity was assessed with two insertions of *GAL4* in the *fru* locus (Fig. 7, b and c). The *fruGAL4A* allele is a targeted insertion that fuses GAL4 to the N-terminus of the male specific isoforms, and results in a decrease in male fertility and courtship (Fig. 7b, $P < 0.0001$) (Stockinger *et al.* 2005). The *fruGAL4B* allele is an insertion of a *GAL4* enhancer detector in *fru* that strongly reduced male fertility and courtship (Fig. 7c, $P < 0.0001$) (Kimura *et al.* 2005). Using *fruGAL4A* to screen the effect of expression of 13 nonresident TFs on fertility, expression of DISCO rescued male fertility. The *fruGAL4A* allele over fru^{4-40} reduced the fertility to 50%, and expression of DISCO increased this fertility to 90% ($P < 0.0001$) (Fig. 7b). The fertility rescued by expression of DISCO was not different from wild type or the fru^{4-40} heterozygote ($P > 0.05$; Fig. 7b). The *fruGAL4B* allele strongly reduced fertility and expression of DISCO was the only protein that increased the fertility, although not significantly, to 14% ($P = 0.8$) (Fig. 7c). Repeating the expression of DISCO in *fruGAL4B*/fru^{4-40} with a larger sample size showed an increase in the fertility ($P < 0.003$) relative to *fruGAL4B*/fru^{4-40} (Fig. 7f). However, the increased fertility observed with expression of DISCO in *fruGAL4B*/fru^{4-40} was less than the fertility of wild type and the y; fru^{4-40} heterozygote ($P < 0.0001$) (Fig. 7, c and f) indicating partial rescue of male behavior.

To further characterize the rescue of the fru phenotype by DISCO, male–female (M/F) and male–male (M/M) courtship indices (CIs) were determined (Fig. 7, d and e). The M/F CI was lower with *fruGAL4A*/fru^{4-40} and y; *fruGAL4B*/fru^{4-40} males than with wild type, fru^{4-40}/+ and y; fru^{4-40}/+ males ($P < 0.0001$). The M/F CI of *P{UAS-disco, w+}*; *fruGAL4A*/fru^{4-40} males was not different from wild type ($P = 0.7$) and fru^{4-40}/+ heterozygous males ($P = 1$), and higher than *fruGAL4A*/fru^{4-40} males ($P = 0.0007$) indicating that DISCO rescued the *fruGAL4A*/fru^{4-40} courtship phenotype. However, expression of DISCO did not rescue the CI of *fruGAL4B*/fru^{4-40} ($P = 0.1$; however, $P = 0.05$ if the CI of *fruGAL4B*/fru^{4-40} is set as the control as opposed to an analysis of all pairwise comparisons), but there is an increase in the magnitude of the CI to a level in line with *fruGAL4A*/fru^{4-40} that has a similar level of fertility as *P{UAS-disco, w+}*; *fruGAL4B*/fru^{4-40} (Fig. 7 f). *fruitless* alleles are reported to have a higher M/M CI (Demir and Dickson 2005). We observed relative to wild-type males a higher M/M courtship of y; fru^{4-40}/+, fru^{4-40}/+, y; *fruGAL4B*/fru^{4-40} and *fruGal4A*/fru^{4-40} males and when DISCO was expressed in either *fruGAL4B*/fru^{4-40} or *fruGal4A*/fru^{4-40} males. The high M/M CI of y; fru^{4-40}/+ *and* fru^{4-40}/+ males made it difficult to interpret the effect of expression of DISCO on the M/M CI in our experiments.

There are three major well-characterized FRU^M protein isoforms: isoform A (FRU^{MA}), isoform B (FRU^{MB}) and isoform C (FRU^{MC}) (Neville *et al.* 2014; von Philipsborn *et al.* 2014). To test whether FRU^{MC} rescues fertility and whether DISCO is a TF required for fertility and activated by FRU^M, the fertility of 11 genotypes were assessed (Fig. 7f). The expression of *UAS-*fru^M (expressing FRU^{MC}) failed to rescue the fertility of hemizygous *fruGAL4A*/fru^{4-40} and *fruGAL4B*/fru^{4-40} males showing that FRU^{MC} is not sufficient for male fertility as might be expected from the redundancy observed with the three isoforms (Fig. 7f)

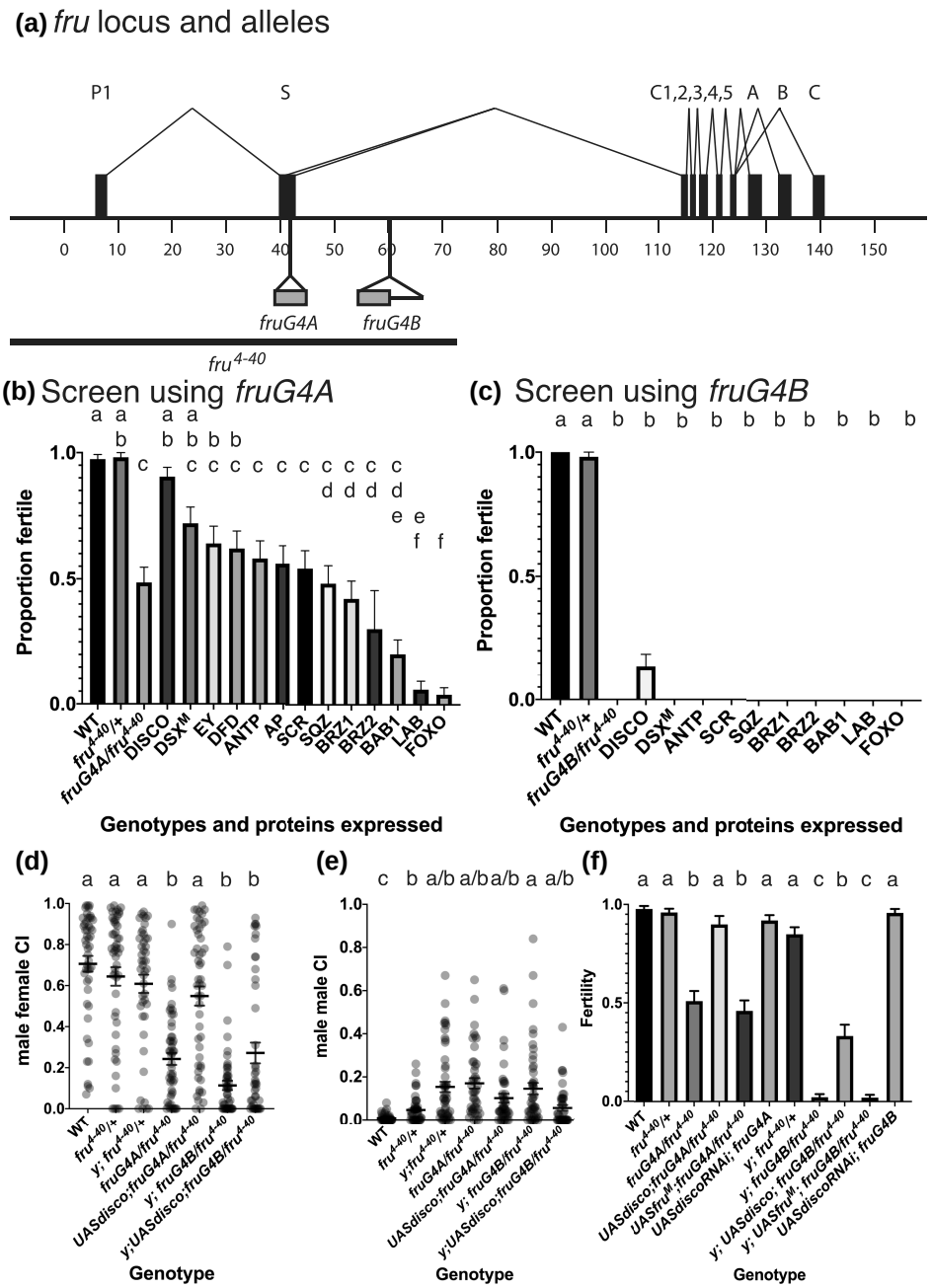

Fig. 7. Summary of the screen for rescue of the fru fertility and courtship phenotypes. (a): The *fru* locus with the insertion site of *fruGAL4A* (*fruG4A*) and *fruGAL4B* (*fruG4B*) and deletion associated with fru^{4-40} indicated. *P1* is one of the alternative promoters of the *fru* gene, S is the sex-specifically spliced exon found only in P1 transcripts. C1-C5 are common exons and A–C are alternative 3′ exons. Panel (b) is a bar graph of the fertility of *fruGAL4A*/fru^{4-40} adult males expressing no protein or the indicated protein. An ANOVA on ranks detected differences [H (15) = 272.8, $P < 0.0001$], and the pair-wise comparisons using Dunn's multiple comparisons analysis that were not different are indicated with the same letter ($P > 0.05$). Panel (c) is a bar graph of fertility of *fruGAL4B*/fru^{4-40} adult males expressing no protein or the indicated protein. An ANOVA on ranks detected differences (H (12) = 620.2, $P < 0.0001$) and the pair-wise comparisons using Dunn's multiple comparisons analysis that were not different are indicated with the same letter ($P > 0.05$). Panels (d) and (e) are scatter plots with means and SEM indicated of male–female (M/F) courtship index (CI) (d) and male–male (M/M) CI (e) for various genotypes (indicated on the x-axis), respectively. An ordinary ANOVA (For M/F CI: $F_{6, 336} = 32$, $P < 0.0001$; for M/M CI: $F_{6, 217} = 7$, $P < 0.0001$) detected differences, and data that are not different ($P > 0.05$) have the same letter after Tukey's multiple comparisons (analysis of the same data with an ANOVA on ranks does not change the conclusions). Panel (f) is a bar graph with SEMs of male fertility in various genotypes indicated on the x-axis. An ANOVA on ranks detected differences [H (10) = 558, $P < 0.0001$], and the pair-wise comparisons using Dunn's multiple comparisons analysis that were not different are indicated with the same letter ($P > 0.05$).

(Neville *et al.* 2014; von Philipsborn *et al.* 2014). Knocking down DISCO expression in FRU expressing cells using *DISCO* RNAi *(TRiP.JF03074)* did not decrease fertility providing no evidence that DISCO is downstream of FRU^M in the male behavior pathway (Fig. 7f).

Doublesex

The *dsx* locus encodes two TFs with distinct activities: DSX^M suppresses the formation of female genitals and promotes sex comb formation, and DSX^F suppresses the formation of male genitals and sex combs and promotes female abdominal pigmentation

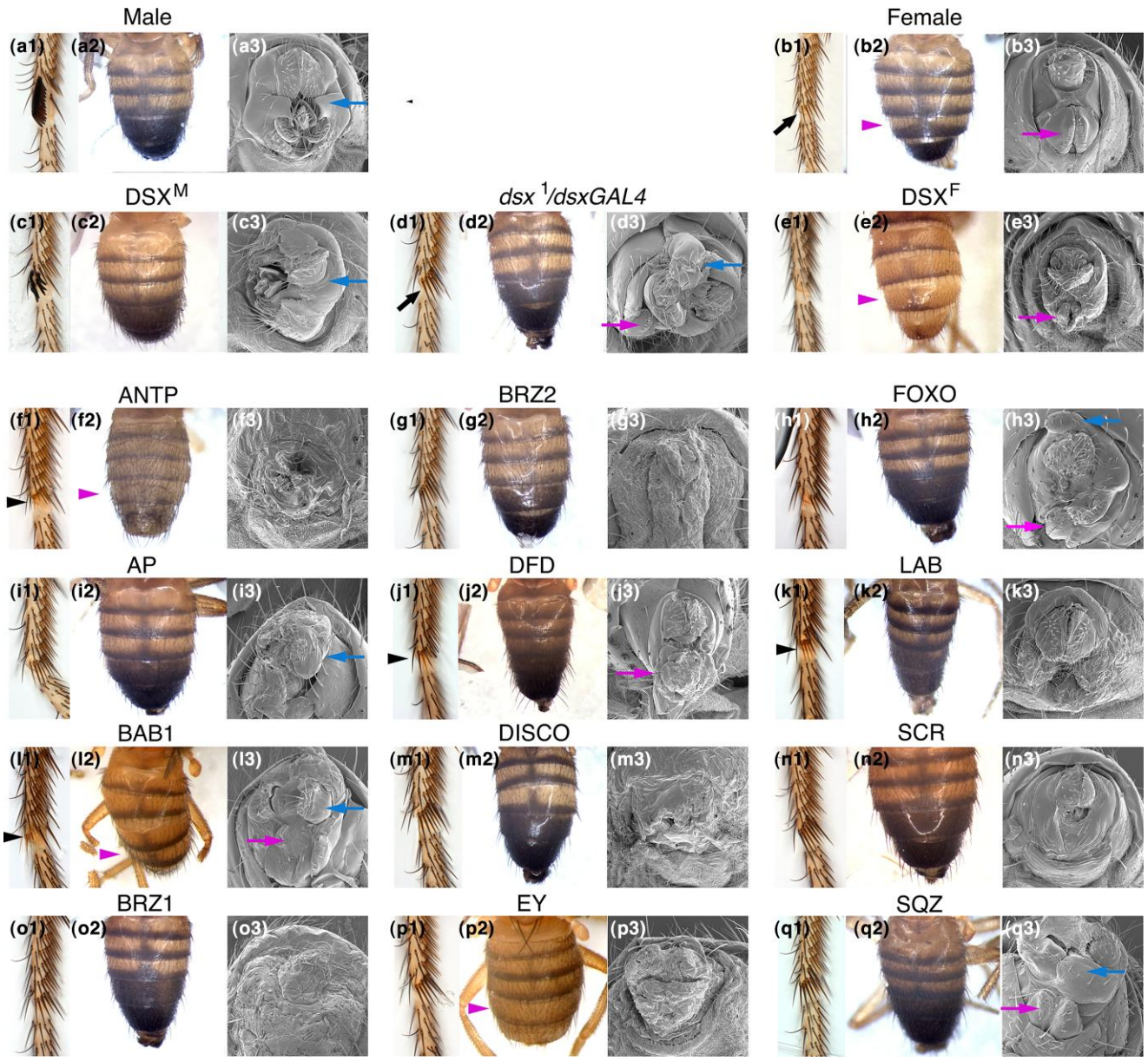

Fig. 8. Screen of 12 TFs for rescue of dsx phenotypes. Each panel is composed of three images: first leg (1), abdomen (2), and genitals (3). Panels (a) and (b) are wild-type male and female flies, respectively. Panel (d) is a $dsx^1/dsxGAL4$ mutant flanked by panels (c) and (d) which are $dsx^1/dsxGAL4$ flies expressing either DSX^M or DSX^F protein, respectively. Panels (f)–(q) are $dsx^1/dsxGAL4$ flies expressing one of 12 TFs indicated above the panel. Pink arrowheads indicate female pigmentation of abdomen. Blue arrows indicate male genitals and pink arrows indicate female genitals. Black arrowheads indicate depigmented sex combs. The black arrow in panel (b1) indicates the five female bristles and in panel (d1) indicates the partially rotated row of sex comb bristles.

(Baker and Ridge 1980; Burtis and Baker 1989). The external somatic secondary sexual characteristics examined in this study were male sex combs, abdominal pigmentation, and genitalia. The male sex combs are a vertical row of about 10–12 darkly pigmented thick bristles with rounded tips (Fig. 8, a1); in females two horizontal rows of approximately five lightly pigmented, spike-like bristles are the equivalent bristles (Fig. 8, b1) (Tanaka *et al.* 2009). In a dsx^{null} mutant, the five lightly pigmented, spike-like female bristles are organized into a single row that is partially rotated toward the vertical (Fig. 8, d1). The important male specific phenotypes of sex combs are an increase in bristle number, a vertical orientation, a change in morphology (rounded tips instead of spike-like) and dark pigmentation (Fig. 8, a1). The tergites 5 and 6 of the male abdomen and the dsx^{null} mutant are fully pigmented (Fig. 8, a2 and d2); whereas, only the posterior portion of tergite 5 and most of tergite 6 are pigmented in females (Fig. 8, b2). The male genitalia are a genital ridge wrapped round the anus and characteristic claspers (Fig. 8, a2); whereas, the female genitals located under the anus is a vaginal plate decorated either side of the vagina with a single row of distinctive bristles, the vaginal teeth (Fig. 8, b3). In dsx^{null} mutants, the genitalia are rotated 90° relative to the dorsal ventral axis and both male and female genitalia form (Fig. 8, d3).

We used the targeted insertion of *GAL4* in the *dsx* locus, which is also a dsx^{null} allele, to express TFs in a $dsxGAL4/dsx^1$ mutant background (Robinett *et al.* 2010). Expression of DSX^M from a *UAS* promoter rescued the vertical orientation, morphology, and pigmentation of sex combs; however, only 4.2 shortened sex

Table 1. Number and type of sex combs associated with expression using *dsxGAL4*.

Protein expressed	Male			Sex neutral (*dsxGal4/dsx*^{1})			Female		
	Male	Sex neutral	Female	Male	Sex neutral	Female	Male	Sex neutral	Female
Control	10.7 ± 0.3 (14)	0 (14)	0 (14)	0 (17)	5.4 ± 0.1 (17)	0 (17)	0 (14)	0 (14)	5.3 ± 0.1 (14)
DSX^{M}	1.9 ± 0.2 (10)^{d}	0 (10)	0 (10)	4.2 ± 0.2 (10)^{d}	0 (10)^{d}	0 (10)	2.9 ± 0.4 (8)^{d}	0 (8)	0 (8)^{d}
DSX^{F}	0 (10)^{d}	0 (10)	5.2 + 0.1 (10)	0 (12)	0 (12)^{d}	5.3 ± 0.1 (12)	0 (13)	0 (13)	5.3 ± 0.1 (13)
ANTP	3.8 ± 0.2 (10)^{d}	0 (10)	0 (10)	0 (16)	6.3 ± 0.2 (13)^{c}	0 (16)	0 (10)	0 (10)	6.3 ± 0.2 (10)^{d}
AP	7.8 ± 0.2 (15)^{d}	0 (15)	0 (15)	0 (19)	6.3 ± 0.1 (19)^{c}	0 (19)	0 (15)	0 (15)	5.1 ± 0.1 (15)
BAB1	9.0 ± 0.2 (6)^{c}	0 (6)	0 (6)	0 (10)	5.4 ± 0.2 (10)	0 (10)	0 (10)	0 (10)	4.7 ± 0.2 (10)
BR.Z1	10.7 ± 0.4 (11)	0 (10)	0 (10)	0 (16)	5.3 ± 0.2 (16)	0 (16)	0 (12)	0 (12)	4.8 ± 0.2 (19)
BR.Z2	9 ± 0.2 (15)^{d}	0 (15)	0 (15)	0 (17)	5.1 ± 0.2 (17)	0 (17)	0 (16)	0 (16)	4.5 ± 0.1 (16)^{b}
DFD	10.8 ± 0.5 (8)	0 (8)	0 (8)	0 (14)	5.4 ± 0.1 (14)	0 (14)	0 (9)	0 (9)	5.1 ± 0.3 (9)
DISCO	9.4 ± 0.2 (12)^{b}	0 (12)	0 (12)	0 (12)	5.4 ± 0.2 (12)	0 (12)	0 (12)	0 (12)	3.7 ± 0.2 (12)^{d}
EY	8.6 ± 0.2 (15)^{d}	0 (15)	0 (15)	0 (15)	5.2 ± 0.2 (12)	0 (12)	0 (12)	0 (12)	4.2 ± 0.3 (19)^{d}
FOXO	10.6 ± 0.3 (10)	0 (10)	0 (10)	0 (10)	4.9 ± 0.2 (10)	0 (10)	0 (12)	0 (12)	5.1 ± 0.2 (12)
LAB	6.3 ± 0.5 (15)^{d}	0 (15)	0 (15)	0 (18)	5.2 ± 0.2 (18)	0 (18)	0 (17)	0 (17)	5.2 ± 0.1 (17)
SCR	10.5 ± 0.3 (12)	0 (12)	0 (12)	0 (13)	4.7 ± 0.1 (13)^{a}	0 (13)	0 (10)	0 (10)	4.8 ± 0.2 (10)
SQZ	10.9 ± 0.2 (18)	0 (18)	0 (18)	0 (13)	5.4 ± 0.1 (13)	0 (13)	0 (15)	0 (15)	5.0 ± 0.1 (15)

The differences from controls in all columns are indicated by asterisks $^{a}P < 0.05$, $^{b}P < 0.01$, $^{c}P < 0.001$, $^{d}P < 0.0001$.

combs form indicating partial rescue (Fig. 8, c1). Tergites 5 and 6 of the abdomen were pigmented (Fig. 8, c2), and development of the vagina was suppressed and male genitalia develop but were rotated indicating partial rescue (Fig. 8, c3). Expression of DSX^{F} from a *UAS* promoter rescued the morphology of the female genitalia; female vaginal plates formed with each plate having two rows of vaginal teeth (Fig. 8, e3). Tergite 5 has female-like pigmentation (Fig. 8, e2), the pigmentation was restricted to the very posterior edge of the segment, and most of tergite 6 was depigmented unlike in wild-type females (Fig. 8, e2).

We screened the expression of 12 TFs for masculinization or feminization of the dsx null phenotype. The observed rescues exhibited differential pleiotropy. *Masculinization*: Expression of ANTP and AP increased the number of sex comb bristles from 5.4 to 6.3 ($P < 0.001$) (Fig. 8, f1 and i1; Table 1). Expression of AP suppressed vagina formation (Fig. 8, i3). *Feminization*: The major phenotypes associated with feminization are suppression of the vertical orientation, number, pigmentation and morphology of sex comb bristles, the pigmentation of the abdomen and the suppression of male genitalia. Expression of ANTP, BAB1, DFD, and LAB depigmented the sex combs (Fig. 8, f1, l1, j1, and k1). LAB repressed the vertical orientation of the sex combs (Fig. 8, k1); the sex combs had a horizontal rather than vertical orientation and were shorter. Expression of ANTP, BAB1, and EY suppressed abdominal pigmentation in the anterior portion of tergites 5 and 6; although ANTP also suppressed abdominal pigmentation overall (Fig. 8, f2, l2, and p2). Expression of BAB1 and FOXO partially suppressed male genitalia but did not delete the vaginal plate (Fig. 8, l3 and h3). DFD, LAB, and SCR suppressed male genitalia and DFD transformed the vaginal plate, whereas the vagina was not observed with expression of LAB and SCR (Fig. 8, j3, k3 and n3). Expression of SQZ increased the number of rows of vaginal teeth (Fig. 8, q3). *Nonspecific*: The genitalia are lost or unrecognizable with expression of ANTP, BR.Z1, BR.Z2, DISCO, and EY.

The *dsx* dominant mutation alleles, *dsx*^{dom}, constitutively express DSX^{M} (Nagoshi and Baker 1990). Expression of DSX^{M} in females by these dominant gain-of-function alleles results in an intersex phenotype similar to the dsx null phenotype; a few sex combs with a dsx null morphology and orientation and development of both male and female genitals. The intersex phenotype in females is hypothesized to be due to DSX^{M} inhibiting the function of DSX^{F}. Likewise when DSX^{F} is ectopically expressed in males, the intersex phenotype is also observed (Waterbury *et al.* 1999). When *dsxGAL4* was used to express DSX^{M} in females, two to four sex combs formed on the first leg that were shorter than normal but were rotated, pigmented, and had rounded tips; the abdomen was pigmented in tergites 5 and 6, and the female genitals were absent and rotated male genitals form (Fig. 9, b4–6). Unexpectedly, when *dsxGAL4* was used to express DSX^{M} in males, only two to three sex combs formed on the first leg that were shorter than normal but were rotated, pigmented, and had rounded tips. The abdomen was pigmented in tergites 5 and 6, and the male genitals were affected with the genital ridge and claspers not fully formed (Fig. 9, b1–b3). When *dsxGAL4* was used to express DSX^{F} in males, the bristles on the first leg were female like, male genital formation was suppressed, and the vaginal plate was present but lacked vaginal teeth (Fig. 9, a1–a3). Expression of DSX^{F} in females reduced abdominal pigmentation (Fig. 9, a5). In summary, expression of DSX^{M} with *dsxGAL4* in females resulted in a male-like phenotype and not an intersex phenotype, and likewise, expression of DSX^{F} with *dsxGAL4* in males resulted in a female-like phenotype and not an intersex phenotype.

Screening the 12 TFs for affects in males and females detected an array of interactions. Expression of ANTP, AP, BAB1, BRZ2, DISCO, EY, and LAB in males suppressed the number of sex combs that form as was observed with both DSX^{M} and DSX^{F} (Fig. 9, c1, d1, e1, f1, i1, j1, and l1; Table 1). Expression of ANTP, BAB1, BRZ1, DFD, DISCO, LAB, and SCR in males depigmented the sex combs as was observed with the expression of DSX^{F} (Fig. 9, c1, e1, f1, h1, i1, l1, and m1). Expression of LAB in males, the sex combs were not rotated toward the vertical as was observed with the expression of DSX^{F} (Fig. 9, l1). Expression of ANTP, BRZ1, and LAB shorten the sex combs as was observed with expression of DSX^{M} in males (Fig. 9, c1, f1, and l1). Expression of BRZ1 feminized the morphology of the sex combs from rounded tips to spikey tips (Fig. 9, f1). Expression of AP, BAB1, SCR, and SQZ in males rotated the male genitals (Fig. 9, d3, e3, m3, and n3). Expression of ANTP, BRZ1, DFD, DISCO, and EY in males deleted the male genitals (Fig. 9, c3, f3, h3, i3, and j3). Expression of FOXO, LAB, and SCR in males reduced the male genitals (Fig. 9, k3, l3, and m3). Expression of ANTP and EY in males depigmented the abdomen overall and tergites 5 and 6 had a female pattern of pigmentation (Fig. 9, c2 and j2). Expression of ANTP, BAB1, and EY in females

Fig. 9. Screen of the expression of 12 TFs in males and females. Two panel sets representing the male and female are given a letter depending on the protein expressed. Male images are 1, 2, and 3; female images are 4, 5, and 6. Each panel is composed of three images: first legs (1/4), abdomen (2/5), and genitals (3/6). Panel (a) is *UAS-dsx*^{F}, *dsxGAL4* male, and female flies. Panel (b) is *UAS-dsx*^{M}, *dsxGAL4* male and female flies. Panels (c)–(n) are *dsxGAL4* flies expressing one of 12 TFs indicated above the panel. Blue arrows indicate rotated and/or reduced male genitals and pink arrows indicate female genitals. Yellow arrow indicates underdeveloped male genitals. Black arrows indicate absent genitals, and green arrows indicate affected female genitals. Black arrowheads indicate depigmented sex combs and pink arrowheads indicate males with depigmented tergite 5.

depigmented most of tergite 6 (Fig. 9, c5, e5, and j5). Expression of ANTP, AP, BRZ1, DISCO, and EY in females resulted in the female genitals not forming (Fig. 9, c6, d6, f6, i6, and j6). Expression of DFD, LAB, and SCR in females did not suppress vagina formation but the morphology was not wild type (Fig. 9, h6, i6, and m6). Expression of SQZ in females increased the number of rows of vaginal teeth (Fig. 9, n6).

The rescue of dsx and effects on male and female development by expression of the 12 TFs exhibit extensive differential pleiotropy as not all somatic sexual phenotypes are affected to the same extent by expression of a nonresident TF (summarized in Table 2). As an example, expression of SCR in males depigments sex combs, but did not reduce the number, rotation or change their morphology, and suppressed male genital formation.

Larger-scale screen for changes in male and female abdominal pigmentation patterns

The examples of ANTP, BAB1, and EY transforming male abdominal pigmentation into a female-like pigmentation pattern, suggested a simple large-scale screen for phenotypic nonspecificity. With the aid of *Dp(1: Y) B*^{s} to mark males with a Bar phenotype, 99 crosses were established representing the expression of 77 TFs using *dsxGAL4*. Of the 77 TFs, 57 were represented once, 18 twice, and 2 thrice. Of the 99 crosses that yielded males, seven [BAB1, hunchback (HB), scalloped (SD), buttonhead (BTD), knirps (KNI), sine occulus (SO), and odd skipped (ODD)] (8%) were found to give reproducible female-like patterns of pigmentation (Fig. 10, d–h). In all seven male cases, the female-like pigmentation pattern was associated with loss of male sex combs and loss of, or

Table 2. Summary of phenotypes of TF (UAS-X) expression in males and females driven by dsxGAL4.

Protein	Males						Females	
	Male sex combs				Genitals	Abdominal Pigmentation	Genitals	Abdominal Pigmentation
	Number	Pigmentation	Rotation	Morphology				
WT	WT	WT	WT	WT	Male	Male	Female	Female
DSX^F	None	depig	No	Female	Female like	Female	Female	Female
DSX^M	Fewer	WT	WT	Shorter	Affected	Male	Male	Male
ANTP	Fewer	depig	Affected	Shorter	Deleted	Female	Deleted	Female
AP	Fewer	WT	WT	WT	Rotated	Male	Deleted	Female
BAB1	Fewer	depig	WT	WT	Rotated	Female	Female	Female
BRZ1	Fewer	depig	WT	Pointed	Deleted	Male	Deleted	Female
BRZ2	WT	WT	WT	WT	Deleted	Male	Deleted	Female
DFD	WT	depig	WT	WT	Reduced	Male	Transformed	Female
DISCO	Fewer	WT	WT	WT	Deleted	Male	Deleted	Female
EY	Fewer	WT	WT	WT	Deleted	Female	Deleted	Female
FOXO	WT	WT	WT	WT	Reduced	Male	Transformed	Female
LAB	Fewer	depig	Affected	Shorter	Reduced	Male	Transformed	Female
SCR	WT	depig	WT	WT	Reduced rotated	Male	Transformed	Female
SQZ	Fewer	depig	WT	WT	Rotated	Male	More teeth	Female

The names of TFs are listed in the column of "Protein". The term "depig" stands for depigmentation.

rotation of, male genitalia but not associated with the formation of a vagina indicating extensive but incomplete feminization. Of the 85 crosses that yielded females, one [Sisterless A (SISA)] (1%) was found to give a reproducible male-like pattern of pigmentation (Fig. 10j). The sex combs of males from 89 crosses were counted in two separate sets depending on whether the males were y+ (Bloomington lines) or y− (Flyorf lines; Bischof *et al.* 2013) (Fig. 10, k and l). Of the 89 counted, 52 had loss of male sex combs; therefore, loss of sex combs was a very common phenotype.

The expression of RNAi molecules using *dsxGAL4* to knock down expression of ANTP, HB, BTD, KNI, SO, SD, ODD, and SISA did not alter male or female abdominal pigmentation providing no evidence that they have a role in wild-type pigmentation and are targets of regulation by DSX^M or DSX^F (Supplementary Fig. S1 f-AC). Loss of function alleles ey^2, sd^1, and so^1 also did not affect abdominal pigmentation (Supplementary Fig. S1). BAB1 and BAB2 are functionally redundant and are required for pigmentation (Couderc *et al.* 2002; Fig. 11).

Epistatic interactions of the expression of ANTP, EY, or HB with *bab1*

DSX^F is required for the expression of BAB1 and BAB2 in females to suppress pigmentation in the posterior tergites of the female (Couderc *et al.* 2002; Williams *et al.* 2008). To test whether the expression of ANTP, EY, and ODD required the expression of BAB1 to suppress pigmentation, ANTP, EY, and ODD were expressed in a *bab1/bab* hemizygous deficiency. Expression of SD, BTD, HB, KNI, and SO could not be assessed because the insertion site on the third chromosome at 86F8 is only three cM away from *dsx*. The *bab1* hemizygous deficiency ($bab1^{Fpa2}/bab^{Ar07}$) that removes both *bab1* genes and one *bab2* gene had a male-like pattern of pigmentation in females (Fig. 11b). The inclusion of this bab^1/bab deficiency in a $dsxGal4/dsx^1$ mutant background did not alter the male like pigmentation of the *dsx* mutant (Fig. 11d). Expression of DSX^F in a $bab1\ dsx^1$ mutant resulted in a male-like pigmentation pattern; therefore, *bab1* is epistatic to DSX^F suggesting that DSX^F is upstream regulating BAB1 expression required for female pigmentation (Fig. 11f) (Williams *et al.* 2008). Expression of BAB1 in a $bab1\ dsx^1$ mutant showed rescue of the bab phenotype to female-like pigmentation (Fig. 11j). Expression of ANTP, EY, or ODD were epistatic to *bab1* rescuing the bab phenotype suggesting either functional complementation of *bab1* or functional complementation of a TF that functions downstream of BAB1 in promoting female pigmentation (Fig. 11, l, n, p, and q).

Apterous

The expression of the AP TF in the dorsal compartment of the wing imaginal disc is required for wing development: loss-of-function alleles in *ap* result in a loss of the wing (Fig. 12a) (Cohen *et al.* 1992). The expression of AP from *UASap* driven by *apGAL4* in an *ap* null mutant rescued wing development (Fig. 12b). The rescue of the ap phenotype by AP was strong in most individuals; however, some wings were not completely rescued indicating that AP was not overexpressed. In an initial screen of expression of 21 nonresident TFs in a *y w; ap^{DG3}/apGAL4; UASTF* genotype only 9 of the 21 (43%) survived to adulthood to be assessed for rescue, and no rescue was observed (Bieli *et al.* 2015) (Supplementary Table 3). AP is also expressed during embryogenesis and required for neurogenesis (Cohen *et al.* 1992). To avoid embryonic lethality due to expression of the nonresident TF in AP expressing embryonic cells, a second screen was performed with 59 nonresident TFs in the *y w; $ap^{MIO1996\text{-}FLPSTOP.D}$/apGAL4; UASTF/$GAL80^{ts}$* genotype (Fisher *et al.* 2017). Embryos and first instar larvae were raised at 23 °C and transferred to 29 °C to inactivate GAL80. 42 (71%) survived to adulthood and could be screened for rescue (Supplementary Table 3). Expression of Caudal (CAD), Tramtrack (TTK), and Myb oncogene-like (MYB) partially rescued the ap wing phenotype giving a phenotype similar to *ap* hypomorphic alleles: all three nonresident TFs rescued wing outgrowth, CAD and TTK rescued wing veins but none rescued formation of the anterior margin bristles (Fig. 12, c–e). Expression of TTK disrupted normal wing development (Fig. 12, f and g). In the 57 crosses that had appropriate progeny to screen, 5 expressed the same TF, and therefore, of 52 different TFs successfully screened, 3 rescued the ap phenotype (6%). Using RNAi to knockdown the expression of CAD *(TRiP.HMS01181)*, MYB *(TRiP.HMS01467)*, and TTK *(TRiP.JF02088)* in AP expressing cells, only knockdown of MYB expression resulted in a wrinkled,

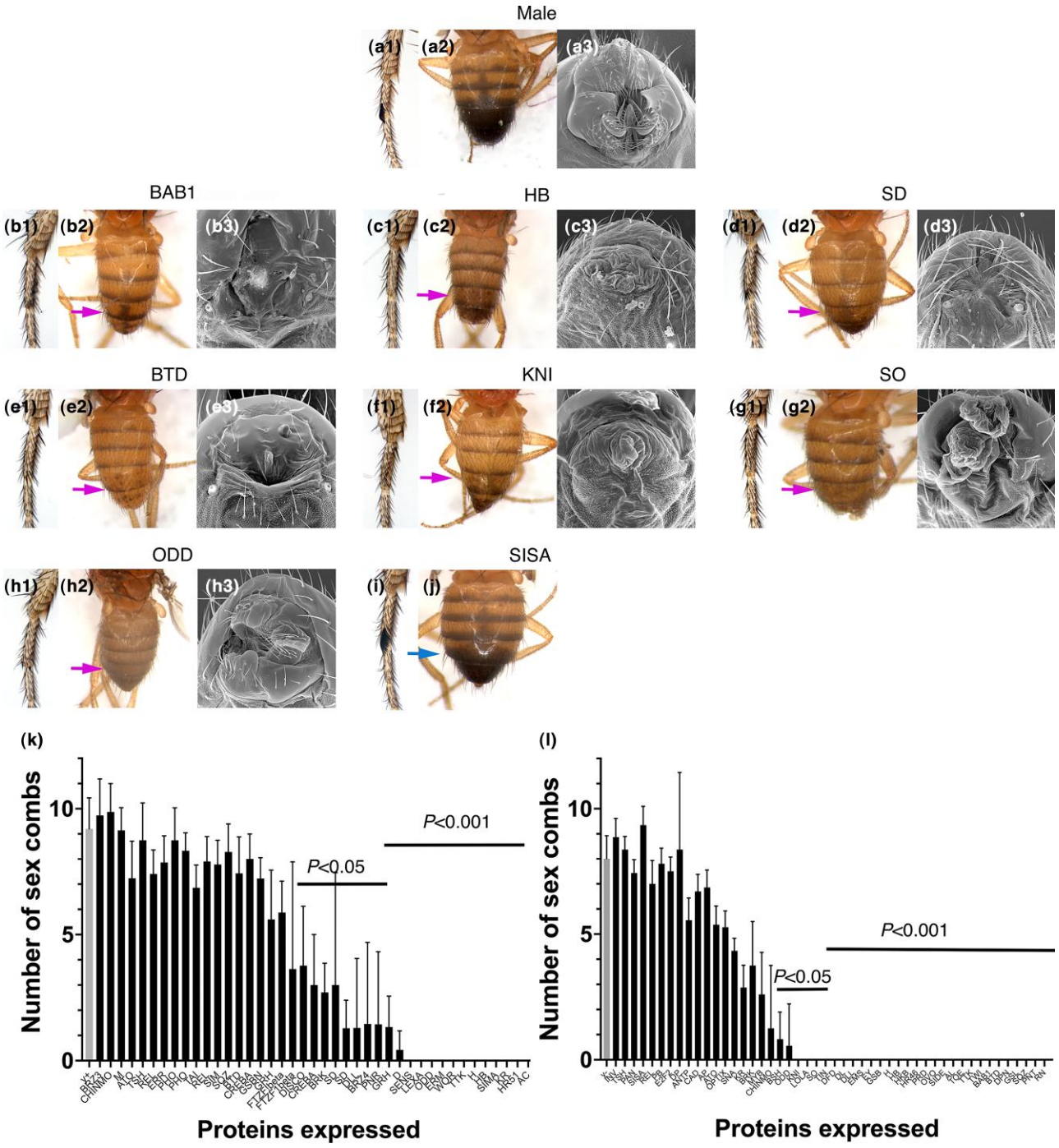

Fig. 10. Phenotypic nonspecificity of abdominal male and female pigmentation and sex comb formation. Panels (a)–(h) are composed of three images from male flies: first legs (1), abdomen (2), and genitals (3). Panel (a) is a wild-type male. The protein expressed by *dsxGAL4* is indicated above the panels (b)–(j). Large scale screens for changes to male and female abdominal pigmentation identified seven TFs that altered male pigmentation (b–h) and one (SISA) that altered female pigmentation but not male sex comb formation (i, j). Panel (i) is a male first leg expressing SISA, and panel (j) is a female abdomen expressing SISA. Female pigmentation of tergite 5 in males is indicated with a pink arrow and male pigmentation of tergite 5 in females is indicated with a blue arrow. Panels (k) and (l) are bar graphs of male first leg sex comb numbers expressing a variety of TFs the SEM is indicated by the error bars. Panel (k) are counts of y^+ sex combs, and panel (l) are the counts of y^- sex combs. An ANOVA of ranks [K H (41) = 384, $P < 0.0001$; L H (48) = 440, $P < 0.0001$] detected differences and the data analyzed with a Dunn's multiple comparison. In both graphs, differences from the control with a P value <0.05 but >0.001 are indicated with a bar and differences with a P value <0.001 are indicated with a second higher bar.

blistered wing phenotype suggesting a role for MYB in normal wing development and may be a potential candidate TF that functions downstream of AP in the wing developmental pathway (Fig. 12h; Supplementary Fig. S1, d and e) (Rovani *et al.* 2012; Rotelli *et al.* 2019).

Discussion

Rescue is not dependent on DNA-binding sequence recognition of TFs

With the exception of ANTP rescuing Ubx, DNA-binding sites recognized by nonresident TFs that rescue TF phenotypes are

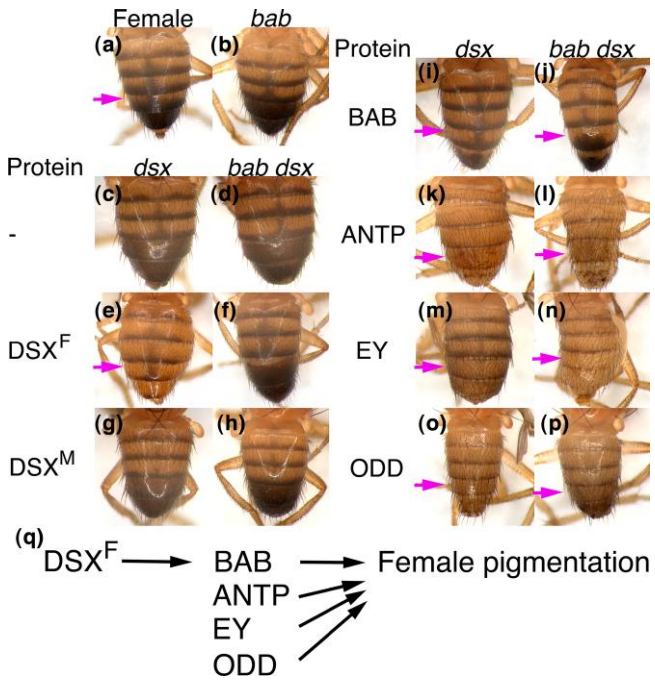

Fig. 11. Expression of ANTP, BAB1, EY, and ODD rescue the bab1 phenotype. a) Wild type. B) *babΔ/bab1*. c) *w; dsxGAL4/dsx*^{1}. d) *w; babΔ dsxGAL4/bab1 dsx*^{1}. e) *w; dsxGAL4/dsx*^{1}, *P{UASdsx*^{F}*}*. f) *w; babΔ dsxGAL4/bab1 dsx*^{1}, *P{UASdsx*^{F}*}*. g, i, k, m, o) *w; P{UASX}; dsxGAL4/dsx*^{1} where X is the gene expressing the protein indicated to the left of the panel. h, j, l, n, p) *w; P{UASX}; babΔ dsxGAL4/bab1 dsx*^{1} where X is the gene expressing the protein indicated to the left of the panels. The pink arrows in panels (a), (e), (i)–(p) point to female-like abdominal pigmentation. q) Diagram of the epistatic relationships between the expression of DSX^{F}, ANTP, EY, and ODD with *bab1/babΔ* on female pigmentation.

distinct from one another and distinct from the DNA recognition site of the resident TF (Fig. 13). Interestingly, expression of a single DISCO protein rescues the fru phenotype that is proposed to require the expression of three FRU^{M} protein isoforms that recognize three very distinct DNA binding sites (Neville *et al.* 2014; von Philipsborn *et al.* 2014). The class of TFs that rescue the phenotypes are diverse as well. HD containing TFs (LAB and SCR) are rescued by DM domain containing protein (DSX^{M}) and winged helix domain contain protein (FOXO). DM domain containing protein (DSX^{F}) is rescued by a PAX6 TF (EY), Zn finger containing TFs (HB, ODD), the SIX family of TFs (SO), TEA/ATTS containing TF (SD), nuclear receptor superfamily (KNI), and HD-containing TF (ANTP). BTB Zn finger TFs (FRU$^{MA\text{-}C}$) are rescued by a Zn finger TF (DISCO). LIM HD containing TF (AP) is rescued by a HD containing TF (CAD), a Zn finger TF (TTK), and a helix turn helix TF (MYB). This diversity suggests that although a DNA-binding domain is important to get a TF onto DNA, the DNA sequence recognized is not important. This may be a consequence of the DNA recognition sites of eukaryotic TFs having a low information content, such that in a two kilobase DNA fragment that might encompass a *cis*-regulatory sequence, there is high expectation that one or more binding sites for a particular TF exists; for example, a TF that recognizes 10 bits of information would be expected to bind four times on average in 2 kb regulatory sequence (Wunderlich and Mirny 2009).

Frequency of phenotypic nonspecificity

A goal of this study is to assess the frequency of phenotypic nonspecificity both across TF phenotypes in many small screens and as a reproducible phenomenon for specific phenotypes in large screens. Of the seven *TF* loci assessed, phenotypic nonspecificity was observed in six indicating that phenotypic nonspecificity is a general expectation and not restricted to a small subset of *TF* loci. A method to calculate the frequency of rescue is to consider all *TF* loci and count the number of rescues by a nonresident TF restricting the dsx examples to alterations in abdominal pigmentation. This would be 18 TF rescues out of 308 cases (6%): rescue of lab, Scr, Ubx, and fru by DSX^{M}, FOXO, ANTP, and DISCO, respectively, rescue of dsx female pigmentation by BAB1(twice), ANTP, EY, SD, SO, HB, ODD, KNI, BTD, rescue of male pigmentation by SISA, and rescue of ap mutant wing development by CAD, TTK, and MYB. However, the expression of FOXO driven by *ScrGAL4* and the large-scale screens for changes in abdominal pigmentation should really be considered as induction of phenotypes as opposed to rescue. Restricting the discussion to purely rescue of phenotypes then 10 TFs rescue out of 106 (9%): rescue of lab, Ubx, and fru by DSX^{M}, ANTP, and DISCO, respectively, rescue of dsx female pigmentation by BAB1, ANTP, EY, ODD, and rescue of ap mutant wing development by CAD, TTK, and MYB. This would increase to 11 out of 114 if the rescue of pb by DSX^{M} is included (10%) (Percival-Smith 2017). However, the frequency would increase to 71 of 308 if the loss of male sex combs was included (Fig. 10, k and l) (23%). Conservatively the frequency is between 5% and 10%; therefore, rescue would be expected to occur on average once in every 10–20 TF screened, but to have a 95% confidence in identifying phenotypic nonspecificity the expected mean for the screen would have to be three (Poisson distribution proportion in the zero class of $0.05 = e^{-3}$), and therefore, between 30 and 60 TFs would need to be screened.

The 5–10% frequency is likely low for three reasons. Some TFs were screened twice or more in the dsx and ap screens and variation in the penetrance was observed. Expression of BAB1 from two insertions results in female pigmentation of males; however, only one of two UAS insertions expressing ANTP, EY, HB, or SD resulted in female pigmentation of males. Insertions expressing BAB1, HB, ODD or SD reduced the number of sex combs; however, only one of two insertions of ANTP and EY reduced the number of sex combs. In the ap screen, only one of two insertions expressing TTK rescued. The variation in penetrance of these phenotypes may be due to either position effect variation where the expression of the protein from one insertion is less than the other, or the epitope tags on EY, ANTP, HB, and ODD result in lower activity. Although epitope tagging is thought to be relatively innocuous, tagging SCR with a triple tag or BFP changes the penetrance of some of the pleiotropic phenotypes induced by ectopic expression of SCR (Percival-Smith *et al.* 2013). Finally, most of the *GAL4* drivers used in this study did not drive the expression of the resident TF to a level that resulted in full rescue of the phenotype. The head length of the rescue of lab with LAB was lower than wild type, the rescue of Scr by SCR was lower than wild type both for the number of T1 setae and the number of sex combs, the haltere rescue of Ubx$^{abx1\ bx3\ 61d\ pbx1}$ by UBX was also incomplete (no capitellium), the rescue of Dfd with DFD was very poor, and the rescue of dsx with DSX^{M} was also incomplete both in terms of the number of sex combs and full rescue of the genitalia (the male genitalia are rotated). Since FRU^{MC} does not rescue the fru phenotype, it is difficult to assess how TFs are being expressed using the two *fruGAL4* drivers. Therefore, for six of the seven screens the resident, and presumably the nonresident TFs as well, are underexpressed suggesting that the observed rescues are not an artifact of overexpression of a TF. The only driver used that results in overexpression is the *rnGAL4* that results in a 200 % increase in the number of sex

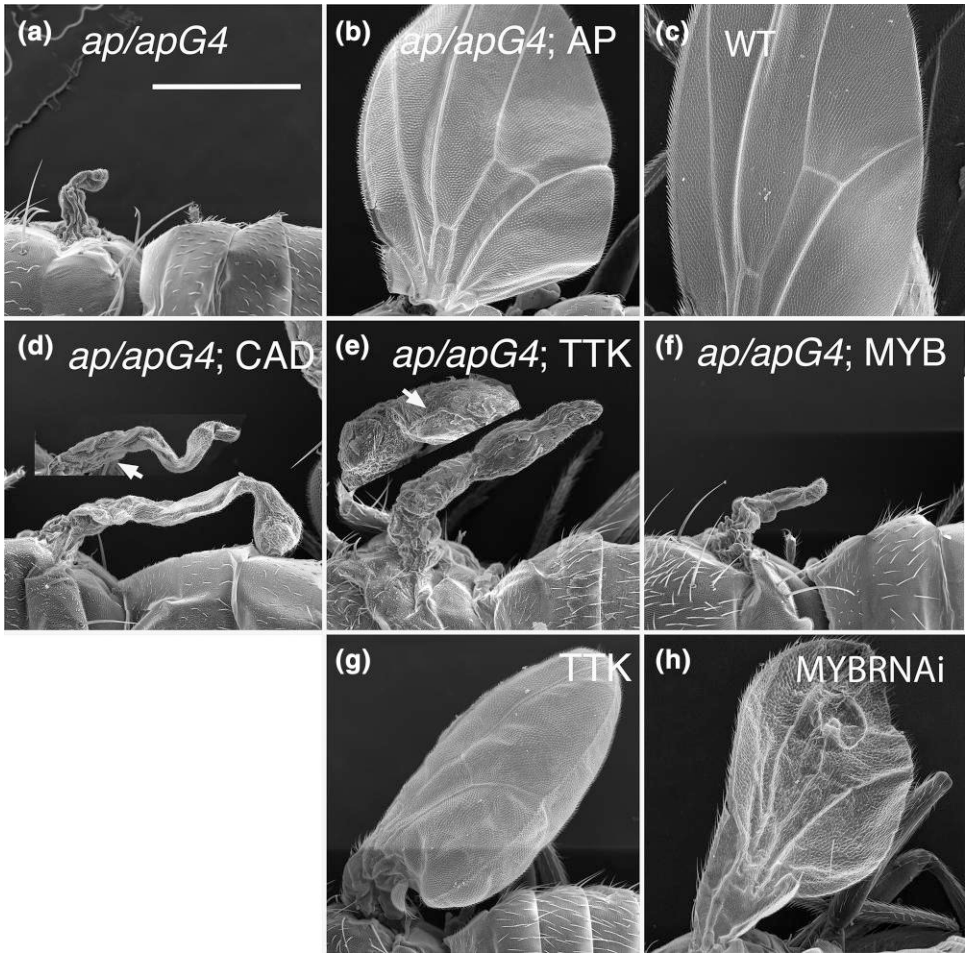

Fig. 12. Rescue of the apterous phenotype by expression of AP, CAD, TTK, and MYB. a) *y w; apGAL4/ap*$^{MIO1996\text{-}FLPSTOP.D.}$. b) *y w; apGAL4/ap*$^{MIO1996\text{-}FLPSTOP.D}$*; P{UASap}/+*. c) Wild type. d) *y w; apGAL4/ap*$^{MIO1996\text{-}FLPSTOP.D}$*/P{UAScad}/+*. The insert in panel d is an independent rescue that has rescue of wing vein tissue (arrow). e) *y w; apGAL4/ap*$^{MIO1996\text{-}FLPSTOP.D}$*/UASttk/+*. The insert in panel e is an independent rescue that has rescue of wing vein tissue (arrow). f) *y w; apGAL4/ap*$^{MIO1996\text{-}FLPSTOP.D}$*; P{UASmyb}/+*. g) *y w apGAL4/+; P{UASttk}/+*. h) *y w; apGAL4; P{UAS TRiP.HMS01467}/+*. The bar in panel a is 500 μm long.

combs on the first leg due to SCR expression (Sivanantharajah and Percival-Smith 2014).

Functional complementation vs epistasis

There are two mechanisms for how expression of a nonresident TF rescues a phenotype. First, true substitution of function of the resident TF (functional complementation). Second, the nonresident TF is a downstream (epistatic) factor positively regulated by the resident TF such that the expression of the nonresident TF independently of the resident TF rescues the phenotype caused by the loss of the resident TF. To address this issue, we determined whether the nonresident TF is required for the phenotype by knocking down its expression. If the nonresident TF has no role in the phenotype assessed, then the rescue cannot be simply the expression of a required epistatic pathway function. Most of these analyses were performed with presumed RNAi knockdowns of expression, which in some cases may not be sufficient to observe a phenotype, but in four (*ey, sd, so, dsx*) of the 18 cases of rescue loss-of-function alleles in the *TF* locus show no role for the TF in the phenotype assessed. Therefore, for 16 of 18 rescues the TF is not required, and in only two cases was there a requirement of the TF in the pathway (BAB1 and MYB). It is clear that BAB1 normally functions downstream of, and is regulated by, DSX^{F}; however, MYB may normally be involved in a wing formation process that is independent of the process associated with AP, and therefore, the rescue of the ap phenotype by MYB may still be functional complementation (Williams *et al.* 2008). The analysis of the epistatic interactions between expression of DSX^{F}, ANTP, EY, ODD showed that ANTP, EY, and ODD are epistatic to *bab1*. This indicates that ANTP, EY, and ODD are not substituting for DSX^{F} in female abdominal pigmentation rather ANTP, EY, and ODD may be substituting for the loss of BAB expression or may function downstream of BAB substituting for another unknown TF with a role in female pigmentation. This latter possibility is unlikely because the gene network for female pigmentation does not include another TF between BAB and expression of the genes required for pigmentation (Roeske *et al.* 2018). Therefore, even though showing that a nonresident TF is not required for the process being assessed supports functional complementation, it does not mean that the nonresident TF is substituting (complementing) for the resident TF function as the nonresident TF could still nonspecifically substitute for a downstream TF that is activated by the resident TF. The demonstration of *cis*-element bypass is required to distinguish between these alternatives.

If the nonresident TF (CAD) is truly substituting for the resident TF (AP) (functional complementation), and the gene regulated by AP is known and then *cis*-element bypass is expected (Percival-Smith 2018). Demonstration of *cis*-element bypass requires showing that

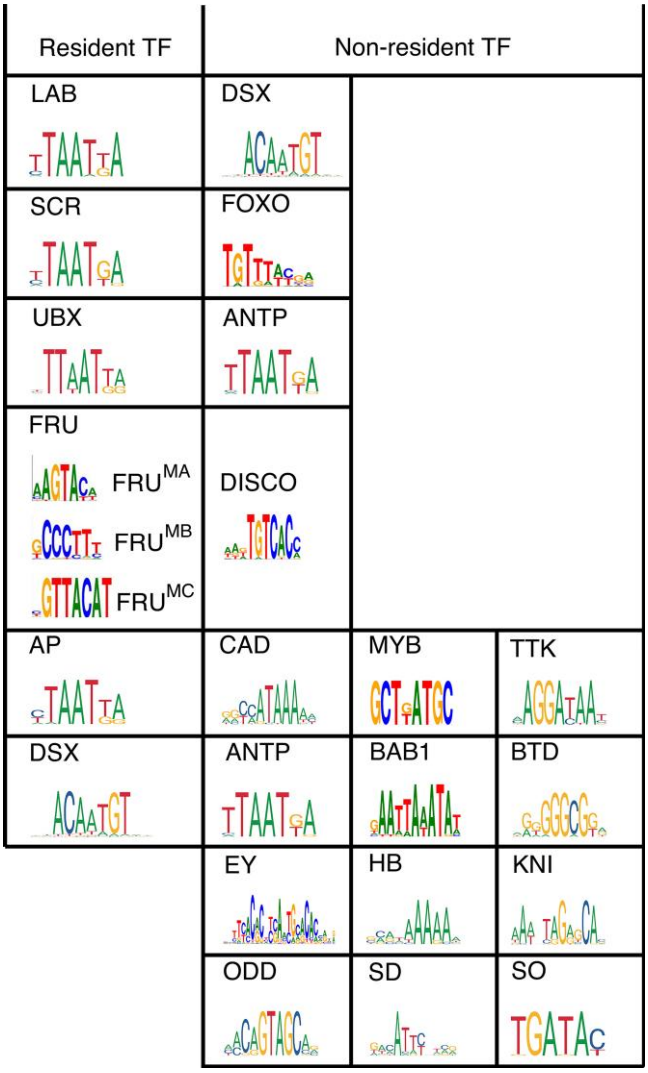

Fig. 13. DNA binding specificity of the resident and nonresident TFs that rescue the phenotypes. The first column on the left shows the DNA-binding sites of the resident TFs as sequence logos. The columns on the right show the DNA-binding sites of the rescuing nonresident TFs. For dsx only, the TF that induce female abdominal pigmentation are represented.

the DNA recognition site for AP in the AP regulated gene is no longer required when CAD is expressed in place of AP, but when CAD is expressed in place of AP the CAD DNA-binding sites would be required for expression of the AP regulated gene. The redundant functional complementation observed with a majority of cases of phenotypic non specificity of trans-acting TF function should also be mirrored in regulatory sequences as redundancy of *cis*-acting regulatory sequences.

Differential pleiotropy of rescue

Differential pleiotropy could have two sources in these experiments. The hypomorphic rescue of the phenotypes with expression of the resident TF from *UAS* suggests that both the resident and nonresident TFs are hypoexpressed. Therefore, hypoexpression could result in differential pleiotropy due to different levels of expression of the TF being sufficient to rescue the different pleiotropic phenotypes. For example, SD when expressed at 50% of wild-type levels is sufficient to bring about female pigmentation and delete the sex combs, but expression at 25% wild-type levels results in unchanged pigmentation but deletion of the sex combs. The second source of differential pleiotropy is that expression of the nonresident TF has the protein function to bring about one phenotype but not the other. Our analysis does not allow distinction between these two mechanisms; although when pleiotropic phenotypes of a *TF* locus are examined, extensive differential pleiotropy is observed suggesting that TFs are composed of short sequence elements that make a small but differential contribution to overall activity of the TF (Bhoite *et al.* 2002; Sivanantharajah and Percival-Smith 2009, 2015).

Evolution of TF function

The generation of redundancy by gene duplication is a major mechanism of evolutionary change (Ohno 1970; Chain and Assis 2021). Phenotypic nonspecificity shares with this hypothesis redundancy of TF function; however, the amino acid sequences of the redundant TFs are dissimilar, indicating that the redundancy is not generated by simple gene duplication. This redundancy allows the exchange of TFs in developmental pathways during evolution. For example, Bicoid is unique to cyclorrhaphan flies and is required for early anterior posterior coordinate determination in Drosophila (Datta *et al.* 2018; Liu *et al.* 2018). A proposal for the evolution of Bicoid is the gradual accumulation of mutations associated with changes in DNA binding specificity. Although this gradual accumulation of mutations explains the data, phenotypic nonspecificity in the future could be considered as a viable alternative for how the function of Bicoid in anterior–posterior coordinate determination arose (Percival-Smith 2018). All insects have anterior ends composed of the head and thorax that are determined by nonconserved mechanisms. Therefore, in a root ancestor of *D. melanogaster*, a TFa, which may have been an ancestral Orthodenticle ortholog, is required for determination of the anterior end exclusively and in a subsequent ancestor Bicoid protein is expressed at the anterior end of the early embryo and at this point TFa and Bicoid (TFb) are functionally redundant for the determination of the anterior end. In the next step in the lineage leading to *D. melanogaster*, expression of TFa at the anterior end is lost and now the development of the anterior end is dependent on expression of Bicoid (TFb). An expectation of this proposal, and not expected in the gradual mutation model, is that Bicoid function can be substituted by many other TFs that recognize distinct DNA-binding sites which would not rule out the gradual mutation model but would support considering phenotypic nonspecificity as a viable alternate explanation.

Although systematic screens for phenotypic nonspecificity with nonresident yeast *S. cerevisiae* TFs have not been performed in *S. cerevisiae*, analysis of the evolution of yeast TF phenotypes provides potential examples of phenotypic nonspecificity. The overall logic of mating type circuit is conserved through evolution of various yeasts, but the TFs that execute the circuit are not orthologs (Tsong *et al.* 2006). The roles of Gal4p, Ppr1p, and Ndt40p in different yeast species are not conserved (Martchenko *et al.* 2007; Askew *et al.* 2009; Tebung *et al.* 2016; Dalal and Johnson 2017; Nocedal *et al.* 2017). Therefore, future potential screens for phenotypic nonspecificity in yeast may identify examples that would support a potential role for phenotypic nonspecificity in the evolution of yeast genetic circuits.

Mechanism of TF function

One of the enduring open questions in the regulation of the initiation of transcription is how, against all odds, TFs find DNA-binding sites on a bacterial chromosome and in eukaryotic chromatin. This is a thermodynamic and informatic question.

The simple model of three-dimensional diffusion of the TF and DNA-binding site is not sufficient to explain this search. From the very beginning, kinetic problems were encountered that led to the proposal of facilitated diffusion (Riggs *et al.* 1970; Hammar *et al.* 2012; Woringer and Darzacq 2018). Also, the observation that low affinity binding sites for TFs are important and the short half-life of TFs bound to their sites in vivo relative to that measured in vitro are difficult to reconcile in the simple diffusion model (Ades and Sauer 1994; Crocker *et al.* 2015; Mir *et al.* 2017; Rastogi *et al.* 2018). Recent analysis of how eukaryotic TFs search the genome for DNA-binding sites has led to a number of proposals that include the TF collective model, pioneer factor hypothesis, the TF funnel model, collaborative competition model, and the two-step nuclear search hypothesis (Mirny 2010; Spitz and Furlong 2012; Castellanos *et al.* 2020; Zaret 2020; Staller 2022). The two-step nuclear search hypothesis explains the phenomena of the intrinsically disordered regions (IDRs) of yeast Msn2p and Yap1p being necessary and sufficient to target the yeast regulatory regions, and therefore, suggesting that the DNA-binding domains of these proteins are somewhat dispensable, as has also been observed with Drosphila Fushi tarazu and EY TFs (Fitzpatrick *et al.* 1992; Hyduk and Percival-Smith 1996; Guichet *et al.* 1997; Punzo *et al.* 2001; Brodsky *et al.* 2020). In the wolf pack version of the two-step nuclear search hypothesis, TFs use their IDRs to form a "protein cloud"/compartment in the nucleoplasm consisting of many different TFs and these TF compartments then search for genomic-binding sites. "Protein cloud" is a loose term for the formation of a nonmembrane bound protein compartment that is not necessarily a protein condensate, or a phase separated compartment, but could be. The wolf pack version of the two-step nuclear search hypothesis will be used to explain phenotypic nonspecificity of TF function.

Both the very specific model for TF function and the model of limited specificity of TF function assume that TFs assemble/are recruited on *cis*-acting DNA-binding sites, but this presumption is not experimentally demonstrated as the mechanism used in vivo (Percival-Smith 2018). Therefore, another possible model is to assume that TFs preassemble/compartmentalize into wolf packs prior to searching for DNA-binding sites (Staller 2022). Drosophila cells express 80–150 TFs (Konstantinides *et al.* 2018; Li *et al.* 2022). We propose the set of TFs expressed in the cell assemble/compartmentalize in the nucleoplasm by partitioning into restricted compartments/protein clouds (wolf packs) of approximately the same size, and the individual compartment of TFs uses all DNA sequence recognition information of the compartmental TFs to search for sets of DNA-binding sites in the genome. The frequency of phenotypic nonspecificity suggests how many compartments, or wolf packs, exist in a cell. Assuming a frequency of 10% then there are 10 compartments in the cell composed of 8–15 different TFs (this calculation assumes that rescue occurs when TFb is partitioned to a specific wolf pack; therefore, to have a frequency of one in 10 there are approximately 10 wolf packs in a cell). The first step for a freshly translated TF is to partition into a wolf pack, and as part of the pack participate in finding DNA sequences to bind. The contribution of an individual TF to the information required for the search of the genome by the pack is small. When TFa is removed from a wolf pack, the wolf pack may not form resulting in a mutant phenotype. In phenotypic nonspecificity, the expression of TFb, which can enter and form the wolf pack, substitutes for TFa but does not have to bind to similar recognition sequences as TFa. This is because the other 7–14 TFs in the pack will lead the TF wolf pack to the same regulatory sequences as with TFa. And, it is likely these regulatory sequences have binding sites for TFb (if you assume that the average eukaryotic TF recognizes five bases of information and that a regulatory sequence has a length in the range of 2 kb then on average a binding site occurs four times). The wolf pack model takes the problem of individual eukaryotic TFs having to search the genome for TF binding sites that have low information content and transforms the low information content of TF binding into a solution for part of an explanation of phenotypic nonspecificity (Wunderlich and Mirny 2009). Also, this wolf pack explanation for phenotypic nonspecificity predicts the experimental expectation of *cis*-element bypass (Percival-Smith 2018) and may explain how a gene is regulated by multiple enhancers (primary and shadow) that generate overlapping expression patterns (Kvon *et al.* 2021). How TFs partition into wolf packs is assumed to be dependent on the set of TFs expressed in a cell; therefore, the partitioning of a specific TF is dependent on the context supplied by the other TFs expressed in the cell. This provides a mechanism for explaining differential pleiotropy as every cell expresses a distinct set of TFs and this sets up different partitioning opportunities for a TF (Sivanantharajah and Percival-Smith 2015). In addition, the wolf pack model is an explanation for phenotypic convergence where multiple TFs can bring about a single phenotype (Konstantinides *et al.* 2018). Although this wolf pack model nicely explains many aspects of phenotypic nonspecificity, there is no direct, unequivocal supporting evidence, but there is also no direct, in vivo evidence that unequivocally supports the recruitment model. Therefore, the strongly held, and most basic, presumptions of the mechanism of regulation of transcription initiation need rigorous experimental tests and future models need to incorporate an explanation of the observation of extensive functional redundancy of TFs.

Data availability

Most of the stocks used in this study are available at indicated Drosophila stock centers (Supplementary Table 2), and any stocks constructed for this study will be made available upon request. The authors affirm that all data necessary for confirming the conclusions of the article are present within the article, figures, and tables.

Supplemental material available at GENETICS online.

Acknowledgments

We thank Ben Rubin for assistance with statistical analysis and Ivan Barker for assistance in SEM. We thank Martin Muller for the ap^{DG3} allele and A.P.-S. thanks Markus Affolter for providing lab space during a sabbatical. SEM was performed at Biotron Integrated Microscopy Laboratory or at Surface Science Western (London, ON). We thank the three reviewers for their helpful suggestions on the manuscript.

Contributions to the paper: A.P.-S. designed the study. A.P.-S. and S.C. established stocks for the lab, Dfd, Scr, Ubx, dsx, and fru small-scale rescue screens. S.C. performed the lab, Dfd, Scr, dsx, and fru screens. A.P.-S. performed the Ubx screen. K.O. performed the large-scale dsx screen. A.P.-S. performed the large-scale screen for rescue of the ap phenotype. A.P.-S. performed the courtship assays and S.C. determined the courtship indexes. A.P.-S. collected all the SEM images and performed all RNAi knockdown experiments. A.P.-S. performed all the statistical analysis of the data. A.P.-S. wrote the first draft of the paper and all authors revised the drafts.

Funding

The research was funded by a Natural Science and Engineering Research Council Discovery Grant awarded to A.P.-S.

Conflicts of interest

The authors declare no conflict of interest.

Literature cited

Abbott MK, Kaufman TC. The relationship between the functional complexity and the molecular organization of the Antennapedia locus of *Drosophila melanogaster*. GENETICS. 1986; 114(3):919–942. doi:10.1093/genetics/114.3.919.

Ades SE, Sauer RT. Differential DNA-binding specificity of the engrailed homeodomain: the role of residue 50. Biochemistry. 1994;33(31):9187–9194. doi:10.1021/bi00197a022.

Anand A, Villella A, Ryner LC, Carlo T, Goodwin SF, Song HJ, Gailey DA, Morales A, Hall JC, Baker BS, *et al.* Molecular genetic dissection of the sex-specific and vital functions of the Drosophila melanogaster sex determination gene fruitless. GENETICS. 2001; 158(4):1569–1595. doi:10.1093/genetics/158.4.1569.

Askew C, Sellam A, Epp E, Hogues H, Mullick A, Nantel A, Whiteway M. Transcriptional regulation of carbohydrate metabolism in the human pathogen *Candida albicans*. PLoS Pathog. 2009;5(10): e1000612. doi:10.1371/journal.ppat.1000612.

Baker BS, Ridge KA. Sex and the single cell. I. On the action of major loci affecting sex determination in *Drosophila melanogaster*. GENETICS. 1980;94(2):383–423. doi:10.1093/genetics/94.2.383.

Bender A, Sprague GF Jr. MAT alpha 1 protein, a yeast transcription activator, binds synergistically with a second protein to a set of cell-type-specific genes. Cell. 1987;50(5):681–691. doi:10.1016/0092-8674(87)90326-6.

Bhoite LT, Allen JM, Garcia E, Thomas LR, Gregory ID, Voth WP, Whelihan K, Rolfes RJ, Stillman DJ. Mutations in the pho2 (bas2) transcription factor that differentially affect activation with its partner proteins bas1, pho4, and swi5. J Biol Chem. 2002;277-(40):37612–37618. doi:10.1074/jbc.M206125200.

Bieli D, Kanca O, Gohl D, Denes A, Schedl P, Affolter M, Müller M. The Drosophila melanogaster mutants apblot and apXasta affect an essential apterous wing enhancer. G3 (Bethesda). 2015;5(6): 1129–1143. doi:10.1534/g3.115.017707.

Bischof J, Björklund M, Furger E, Schertel C, Taipale J, Basler K. A versatile platform for creating a comprehensive UAS-ORFeome library in Drosophila. Development. 2013;140(11):2434–2442. doi: 10.1242/dev.088757.

Brodsky S, Jana T, Mittelman K, Chapal M, Kumar DK, Carmi M, Barkai N. Intrinsically disordered regions direct transcription factor in vivo binding specificity. Mol Cell. 2020;79(3):459–471.e4. doi: 10.1016/j.molcel.2020.05.032.

Burtis KC, Baker BS. Drosophila doublesex gene controls somatic sexual differentiation by producing alternatively spliced mRNAs encoding related sex-specific polypeptides. Cell. 1989;56(6): 997–1010. doi:10.1016/0092-8674(89)90633-8.

Carroll SB. Evo-devo and an expanding evolutionary synthesis: a genetic theory of morphological evolution. Cell. 2008;134(1):25–36. doi:10.1016/j.cell.2008.06.030.

Castellanos M, Mothi N, Muñoz V. Eukaryotic transcription factors can track and control their target genes using DNA antennas. Nat Commun. 2020;11(1):540. doi:10.1038/s41467-019-14217-8.

Chain FJJ, Assis R. BLAST from the past: impacts of evolving approaches on studies of evolution by gene duplication. Genome Biol Evol. 2021;13(7):evab149. doi:10.1093/gbe/evab149.

Cohen B, McGuffin ME, Pfeifle C, Segal D, Cohen SM. Apterous, a gene required for imaginal disc development in Drosophila encodes a member of the LIM family of developmental regulatory proteins. Genes Dev. 1992;6(5):715–729. doi:10.1101/gad.6.5.715.

Cole ES, Palka J. The pattern of campaniform sensilla on the wing and haltere of *Drosophila melanogaster* and several of its homeotic mutants. J Embryol Exp Morphol. 1982;71:41–61.

Couderc JL, Godt D, Zollman S, Chen J, Li M, Tiong S, Cramton SE, Sahut-Barnola I, Laski FA. The bric à brac locus consists of two paralogous genes encoding BTB/POZ domain proteins and acts as a homeotic and morphogenetic regulator of imaginal development in Drosophila. Development. 2002;129(10):2419–2433. doi: 10.1242/dev.129.10.2419.

Crocker J, Abe N, Rinaldi L, McGregor AP, Frankel N, Wang S, Alsawadi A, Valenti P, Plaza S, Payre F, *et al.* Low affinity binding site clusters confer hox specificity and regulatory robustness. Cell. 2015;160(1–2):191–203. doi:10.1016/j.cell.2014.11.041.

Dalal CK, Johnson AD. How transcription circuits explore alternative architectures while maintaining overall circuit output. Genes Dev. 2017;31(14):1397–1405. doi:10.1101/gad.303362.117.

Datta RR, Ling J, Kurland J, Ren X, Xu Z, Yucel G, Moore J, Shokri L, Baker I, Bishop T, *et al.* A feed-forward relay integrates the regulatory activities of Bicoid and Orthodenticle via sequential binding to suboptimal sites. Genes Dev. 2018;32(9–10):723–736. doi: 10.1101/gad.311985.118.

Demir E, Dickson BJ. Fruitless splicing specifies male courtship behavior in Drosophila. Cell. 2005;121(5):785–794. doi:10.1016/j.cell.2005.04.027.

Diederich RJ, Merrill VK, Pultz MA, Kaufman TC. Isolation, structure, and expression of labial, a homeotic gene of the Antennapedia complex involved in Drosophila head development. Genes Dev. 1989;3(3):399–414. doi:10.1101/gad.3.3.399.

Fisher YE, Yang HH, Isaacman-Beck J, Xie M, Gohl DM, Clandinin TR. FlpStop, a tool for conditional gene control in Drosophila. eLife. 2017;6:e22279. doi:10.7554/eLife.22279.

Fitzpatrick VD, Percival-Smith A, Ingles CJ, Krause HM. Homeodomain-independent activity of the fushi tarazu polypeptide in Drosophila embryos. Nature. 1992;356(6370):610–612. doi: 10.1038/356610a0.

Greig S, Akam M. The role of homeotic genes in the specification of the Drosophila gonad. Curr Biol. 1995;5(9):1057–1062. doi:10.1016/S0960-9822(95)00210-7.

Guichet A, Copeland JW, Erdélyi M, Hlousek D, Závorszky P, Ho J, Brown S, Percival-Smith A, Krause HM, Ephrussi A. The nuclear receptor homologue Ftz-F1 and the homeodomain protein Ftz are mutually dependent cofactors. Nature. 1997;385(6616): 548–552. doi:10.1038/385548a0.

Hammar P, Leroy P, Mahmutovic A, Marklund EG, Berg OG, Elf J. The lac repressor displays facilitated diffusion in living cells. Science. 2012;336(6088):1595–1598. doi:10.1126/science.1221648.

Hirth F, Hartmann B, Reichert H. Homeotic gene action in embryonic brain development of Drosophila. Development. 1998;125(9): 1579–1589. doi:10.1242/dev.125.9.1579.

Hittinger CT, Stern DL, Carroll SB. Pleiotropic functions of a conserved insect-specific hox peptide motif. Development. 2005;132-(23):5261–5270. doi:10.1242/dev.02146.

Hyduk D, Percival-Smith A. Genetic characterization of the homeodomain-independent activity of the Drosophila fushi tarazu gene product. GENETICS. 1996;142(2):481–492. doi:10.1093/genetics/142.2.481.

Jenett A, Rubin GM, Ngo TT, Shepherd D, Murphy C, Dionne H, Pfeiffer BD, Cavallaro A, Hall D, Jeter J, *et al.* A GAL4-driver line resource for Drosophila neurobiology. Cell Rep. 2012;2(4):991–1001. doi:10.1016/j.celrep.2012.09.011.

Kimura K, Ote M, Tazawa T, Yamamoto D. Fruitless specifies sexually dimorphic neural circuitry in the Drosophila brain. Nature. 2005;438(7065):229–233. doi:10.1038/nature04229.

Konstantinides N, Kapuralin K, Fadil C, Barboza L, Satija R, Desplan C. Phenotypic convergence: distinct transcription factors regulate common terminal features. Cell. 2018;174(3):622–635.e13. doi:10.1016/j.cell.2018.05.021.

Kvon EZ, Waymack R, Gad M, Wunderlich Z. Enhancer redundancy in development and disease. Nat Rev Genet. 2021;22(5):324–336. doi:10.1038/s41576-020-00311-x.

Lewis EB. Genes and developmental pathways. Am Zool. 1963;3(1):33–56.

Li H, Janssens J, De Waegeneer M, Kolluru SS, Davie K, Gardeux V, Saelens W, David FPA, Brbić M, Spanier K, *et al.* Fly cell atlas: a single-nucleus transcriptomic atlas of the adult fruit fly. Science. 2022;375(6584):eabk2432. doi:10.1126/science.abk2432.

Liu Q, Onal P, Datta RR, Rogers JM, Schmidt-Ott U, Bulyk ML, Small S, Thornton JW. Ancient mechanisms for the evolution of the bicoid homeodomain's Function in fly development. eLife. 2018;7:e34594. doi:10.7554/eLife.34594.

Maekawa M, Yamaguchi K, Nakamura T, Shibukawa R, Kodanaka I, Ichisaka T, Kawamura Y, Mochizuki H, Goshima N, Yamanaka S. Direct reprogramming of somatic cells is promoted by maternal transcription factor Glis1. Nature. 2011;474(7350):225–229. doi:10.1038/nature10106.

Martchenko M, Levitin A, Hogues H, Nantel A, Whiteway M. Transcriptional rewiring of fungal galactose-metabolism circuitry. Curr Biol. 2007;17(12):1007–1013. doi:10.1016/j.cub.2007.05.017.

Merrill VK, Diederich RJ, Turner FR, Kaufman TC. A genetic and developmental analysis of mutations in labial, a gene necessary for proper head formation in *Drosophila melanogaster*. Dev Biol. 1989;135(2):376–391. doi:10.1016/0012-1606(89)90187-5.

Mir M, Reimer A, Haines JE, Li XY, Stadler M, Garcia H, Eisen MB, Darzacq X. Dense bicoid hubs accentuate binding along the morphogen gradient. Genes Dev. 2017;31(17):1784–1794. doi:10.1101/gad.305078.117.

Mirny LA. Nucleosome-mediated cooperativity between transcription factors. Proc Natl Acad Sci U S A. 2010;107(52):22534–22539. doi:10.1073/pnas.0913805107.

Nagoshi RN, Baker BS. Regulation of sex-specific RNA splicing at the Drosophila doublesex gene: cis-acting mutations in exon sequences alter sex-specific RNA splicing patterns. Genes Dev. 1990;4(1):89–97. doi:10.1101/gad.4.1.89.

Neville MC, Nojima T, Ashley E, Parker DJ, Walker J, Southall T, Van de Sande B, Marques AC, Fischer B, Brand AH, *et al.* Male-specific fruitless isoforms target neurodevelopmental genes to specify a sexually dimorphic nervous system. Curr Biol: CB. 2014;24(3):229–241. doi:10.1016/j.cub.2013.11.035.

Nocedal I, Mancera E, Johnson AD. Gene regulatory network plasticity predates a switch in function of a conserved transcription regulator. eLife. 2017;6:e23250. doi:10.7554/eLife.23250.

Ohno S. Evolution by Gene Duplication. Heidelberg: Springer-Verlag; 1970.

Percival-Smith A. Non-specificity of transcription factor function in *Drosophila melanogaster*. Dev Genes Evol. 2017;227(1):25–39. doi:10.1007/s00427-016-0566-z.

Percival-Smith A. Phenotypic nonspecificity as the result of limited specificity of transcription factor function. Genet Res Int. 2018;2018:7089109. doi:10.1155/2018/7089109.

Percival-Smith A, Sivanantharajah L, Pelling JJ, Teft WA. Developmental competence and the induction of ectopic proboscises in *Drosophila melanogaster*. Dev Genes Evol. 2013;223(6):375–387. doi:10.1007/s00427-013-0454-8.

Percival-Smith A, Weber J, Gilfoyle E, Wilson P. Genetic characterization of the role of the two HOX proteins, proboscipedia and sex combs reduced, in determination of adult antennal, tarsal, maxillary palp and proboscis identities in *Drosophila melanogaster*. Development. 1997;124(24):5049–5062. doi:10.1242/dev.124.24.5049.

Perkins LA, Holderbaum L, Tao R, Hu Y, Sopko R, McCall K, Yang-Zhou D, Flockhart I, Binari R, Shim HS, *et al.* The transgenic RNAi project at Harvard Medical School: resources and validation. GENETICS. 2015;201(3):843–852. doi:10.1534/genetics.115.180208.

Punzo C, Kurata S, Gehring WJ. The eyeless homeodomain is dispensable for eye development in Drosophila. Genes Dev. 2001;15-(13):1716–1723. doi:10.1101/gad.196401.

Rastogi C, Rube HT, Kribelbauer JF, Crocker J, Loker RE, Martini GD, Laptenko O, Freed-Pastor WA, Prives C, Stern DL, *et al.* Accurate and sensitive quantification of protein-DNA binding affinity. Proc Natl Acad Sci U S A. 2018;115(16):E3692–E3701. doi:10.1073/pnas.1714376115.

Regulski M, McGinnis N, Chadwick R, McGinnis W. Developmental and molecular analysis of deformed; a homeotic gene controlling Drosophila head development. EMBO J. 1987;6(3):767–777. doi:10.1002/j.1460-2075.1987.tb04819.x.

Riggs AD, Bourgeois S, Cohn M. The lac repressor-operator interaction. 3. Kinetic studies. J Mol Biol. 1970;53(3):401–417. doi:10.1016/0022-2836(70)90074-4.

Rivlin PK, Gong A, Schneiderman AM, Booker R. The role of Ultrabithorax in the patterning of adult thoracic muscles in Drosophila melanogaster. Dev Genes Evol. 2001;211(2):55–66. doi:10.1007/s004270000126.

Robinett CC, Vaughan AG, Knapp JM, Baker BS. Sex and the single cell. II. There is a time and place for sex. PLoS Biol. 2010;8(5):e1000365. doi:10.1371/journal.pbio.1000365.

Roeske MJ, Camino EM, Grover S, Rebeiz M, Williams TM. Cis-regulatory evolution integrated the bric-à-brac transcription factors into a novel fruit fly gene regulatory network. eLife. 2018;7:e32273. doi:10.7554/eLife.32273.

Rotelli MD, Bolling AM, Killion AW, Weinberg AJ, Dixon MJ, Calvi BR. An RNAi screen for genes required for growth of Drosophila wing tissue. G3 (Bethesda). 2019;9(10):3087–3100. doi:10.1534/g3.119.400581.

Rovani MK, Brachmann CB, Ramsay G, Katzen AL. The dREAM/Myb-MuvB complex and grim are key regulators of the programmed death of neural precursor cells at the Drosophila posterior wing margin. Dev Biol. 2012;372(1):88–102. doi:10.1016/j.ydbio.2012.08.022.

Sivanantharajah L, Percival-Smith A. Analysis of the sequence and phenotype of Drosophila sex combs reduced alleles reveals potential functions of conserved protein motifs of the sex combs reduced protein. GENETICS. 2009;182(1):191–203. doi:10.1534/genetics.109.100438.

Sivanantharajah L, Percival-Smith A. Acquisition of a leucine zipper motif as a mechanism of antimorphy for an allele of the Drosophila Hox gene sex combs reduced. G3 (Bethesda). 2014;4(5):829–838. doi:10.1534/g3.114.010769.

Sivanantharajah L, Percival-Smith A. Differential pleiotropy and HOX functional organization. Dev Biol. 2015;398(1):1–10. doi:10.1016/j.ydbio.2014.11.001.

Spitz F, Furlong EE. Transcription factors: from enhancer binding to developmental control. Nat Rev Genetics. 2012;13(9):613–626. doi:10.1038/nrg3207.

Staller MV. Transcription factors perform a 2-step search of the nucleus. GENETICS. 2022;222(2):iyac111. doi:10.1093/genetics/iyac111.

Stockinger P, Kvitsiani D, Rotkopf S, Tirián L, Dickson BJ. Neural circuitry that governs Drosophila male courtship behavior. Cell. 2005;121(5):795–807. doi:10.1016/j.cell.2005.04.026.

Struhl G. A homoeotic mutation transforming leg to antenna in Drosophila. Nature. 1981;292(5824):635–638. doi:10.1038/292635a0.

Takahashi K, Yamanaka S. Induction of pluripotent stem cells from mouse embryonic and adult fibroblast cultures by defined factors. Cell. 2006;126(4):663–676. doi:10.1016/j.cell.2006.07.024.

Tanaka K, Barmina O, Kopp A. Distinct developmental mechanisms underlie the evolutionary diversification of Drosophila sex combs. Proc Natl Acad Sci U S A. 2009;106(12):4764–4769. doi:10.1073/pnas.0807875106.

Tebung WA, Choudhury BI, Tebbji F, Morschhäuser J, Whiteway M. Rewiring of the Ppr1 zinc cluster transcr+iption factor from purine catabolism to pyrimidine biogenesis in the saccharomycetaceae. Curr Biol: CB. 2016;26(13):1677–1687. doi:10.1016/j.cub.2016.04.064.

Tsong AE, Tuch BB, Li H, Johnson AD. Evolution of alternative transcriptional circuits with identical logic. Nature. 2006;443(7110):415–420. doi:10.1038/nature05099.

Villella A, Gailey DA, Berwald B, Ohshima S, Barnes PT, Hall JC. Extended reproductive roles of the fruitless gene in *Drosophila melanogaster* revealed by behavioral analysis of new fru mutants. GENETICS. 1997;147(3):1107–1130. doi:10.1093/genetics/147.3.1107.

von Philipsborn AC, Jörchel S, Tirian L, Demir E, Morita T, Stern DL, Dickson BJ. Cellular and behavioral functions of fruitless isoforms in Drosophila courtship. Curr Biol: CB. 2014;24(3):242–251. doi:10.1016/j.cub.2013.12.015.

Waterbury JA, Jackson LL, Schedl P. Analysis of the doublesex female protein in *Drosophila melanogaster*: role on sexual differentiation and behavior and dependence on intersex. GENETICS. 1999;152(4):1653–1667. doi:10.1093/genetics/152.4.1653.

Weinzierl ROJ, Axton JM, Ghysen A, Akam ME. Ultrabithorax mutations in constant and variable regions of the protein coding sequence. Genes Dev. 1987;1(4):386–397. doi:10.1101/gad.1.4.386.

Wieschaus E, Nusslein-Volhard C. Looking at embryos. In: Roberts DB, editors. Drosophila: A Practical Approach. Oxford : IRL; 1986. p. 199–228.

Williams TM, Selegue JE, Werner T, Gompel N, Kopp A, Carroll SB. The regulation and evolution of a genetic switch controlling sexually dimorphic traits in Drosophila. Cell. 2008;134(4):610–623. doi:10.1016/j.cell.2008.06.052.

Woringer M, Darzacq X. Protein motion in the nucleus: from anomalous diffusion to weak interactions. Biochem Soc Trans. 2018;46(4):945–956. doi:10.1042/BST20170310.

Wunderlich Z, Mirny LA. Different gene regulation strategies revealed by analysis of binding motifs. Trends Genet: TIG. 2009;25-(10):434–440. doi:10.1016/j.tig.2009.08.003.

Zaret KS. Pioneer transcription factors initiating gene network changes. Annu Rev Genet. 2020;54:367–385. doi:10.1146/annurev-genet-030220-015007.

Zeng C, Pinsonneault J, Gellon G, McGinnis N, McGinnis W. Deformed protein binding sites and cofactor binding sites are required for the function of a small segment-specific regulatory element in Drosophila embryos. EMBO J. 1994;13(10):2362–2377. doi:10.1002/j.1460-2075.1994.tb06520.x.

Editor: J. Birchler